Research Report 45

AUGUST, 1958

Experimental Study of Frost Heaving

by Akira Higashi

U. S. ARMY SNOW ICE AND PERMAFROST
RESEARCH ESTABLISHMENT
Corps of Engineers
Wilmette, Illinois

PREFACE

The work reported in this paper was carried out by Dr. Higashi, contract scientist, under the general supervision of Mr. W. K. Boyd, acting chief, Frozen Ground Basic Research Branch, as a part of Project 22.3-3, **Dynamics of frost heaving.**

The author expresses his gratitude to Dr. Henri Bader, Chief Scientist, and Mr. Boyd for their encouragement and assistance in carrying out this work.

The author's thanks are due to Mr. G. Martinez for his measurements of the permeability and grain size analysis of the soil.

Department of the Army Project 8-66-02-004

Manuscript received 10 February 1958

AD Accession No

U. S. Army Snow Ice and Permafrost Research Establishment, Corps of Engineers, Wilmette, Ill.
EXPERIMENTAL STUDY OF FROST HEAVING - Akira Higashi

Research Report 45, Aug 58, 44pp-illus-tables.
DA Proj 8-66-02-004, SIPRE Proj 22.3-3.
Unclassified Report

Laboratory studies on the effects of the soil-temperature regime on the type of ice segregation and the rate of frost heaving are described in detail, and the results are analyzed quantitatively on the basis of thermodynamic and hydraulic theory, assuming that suction is created by ice formation. The heaving rate varied with the type of ice segregation, which in turn depended on the rate of frost penetration. Ice-filament layers or sirloin-type freezing were observed at low penetration rates and concrete-type freezing at high penetration rates. The heaving rate decreased with increasing frost-penetration rate, and varied, in the case of filament-type freezing, according to the amount of sensible heat lost at

(over)

UNCLASSIFIED

1. Soils--Frost action effects
2. Soils--Freezing
I. Higashi, Akira
II. U.S. Army Snow Ice and Permafrost Research Establishment

AD Accession No

U. S. Army Snow Ice and Permafrost Research Establishment, Corps of Engineers, Wilmette, Ill.
EXPERIMENTAL STUDY OF FROST HEAVING - Akira Higashi

Research Report 45, Aug 58, 44pp-illus-tables.
DA Proj 8-66-02-004, SIPRE Proj 22.3-3.
Unclassified Report

Laboratory studies on the effects of the soil-temperature regime on the type of ice segregation and the rate of frost heaving are described in detail, and the results are analyzed quantitatively on the basis of thermodynamic and hydraulic theory, assuming that suction is created by ice formation. The heaving rate varied with the type of ice segregation, which in turn depended on the rate of frost penetration. Ice-filament layers or sirloin-type freezing were observed at low penetration rates and concrete-type freezing at high penetration rates. The heaving rate decreased with increasing frost-penetration rate, and varied, in the case of filament-type freezing, according to the amount of sensible heat lost at

(over)

UNCLASSIFIED

1. Soils--Frost action effects
2. Soils--Freezing
I. Higashi, Akira
II. U.S. Army Snow Ice and Permafrost Research Establishment

AD Accession No

U. S. Army Snow Ice and Permafrost Research Establishment, Corps of Engineers, Wilmette, Ill.
EXPERIMENTAL STUDY OF FROST HEAVING - Akira Higashi

Research Report 45, Aug 58, 44pp-illus-tables.
DA Proj 8-66-02-004, SIPRE Proj 22.3-3.
Unclassified Report

Laboratory studies on the effects of the soil-temperature regime on the type of ice segregation and the rate of frost heaving are described in detail, and the results are analyzed quantitatively on the basis of thermodynamic and hydraulic theory, assuming that suction is created by ice formation. The heaving rate varied with the type of ice segregation, which in turn depended on the rate of frost penetration. Ice-filament layers or sirloin-type freezing were observed at low penetration rates and concrete-type freezing at high penetration rates. The heaving rate decreased with increasing frost-penetration rate, and varied, in the case of filament-type freezing, according to the amount of sensible heat lost at

(over)

UNCLASSIFIED

1. Soils--Frost action effects
2. Soils--Freezing
I. Higashi, Akira
II. U.S. Army Snow Ice and Permafrost Research Establishment

AD Accession No

U. S. Army Snow Ice and Permafrost Research Establishment, Corps of Engineers, Wilmette, Ill.
EXPERIMENTAL STUDY OF FROST HEAVING - Akira Higashi

Research Report 45, Aug 58, 44pp-illus-tables.
DA Proj 8-66-02-004, SIPRE Proj 22.3-3.
Unclassified Report

Laboratory studies on the effects of the soil-temperature regime on the type of ice segregation and the rate of frost heaving are described in detail, and the results are analyzed quantitatively on the basis of thermodynamic and hydraulic theory, assuming that suction is created by ice formation. The heaving rate varied with the type of ice segregation, which in turn depended on the rate of frost penetration. Ice-filament layers or sirloin-type freezing were observed at low penetration rates and concrete-type freezing at high penetration rates. The heaving rate decreased with increasing frost-penetration rate, and varied, in the case of filament-type freezing, according to the amount of sensible heat lost at

(over)

UNCLASSIFIED

1. Soils--Frost action effects
2. Soils--Freezing
I. Higashi, Akira
II. U.S. Army Snow Ice and Permafrost Research Establishment

GPO 814972-2

the freezing interface. The sensible heat loss was 0.62 cal/cm-sec in the case of maximum heaving (7 mm/day); higher values resulted in thermal conditions favoring sirloin-type freezing. The moisture content of frozen soil was found to be related to the heaving ratio, inasmuch as the amount of heaving is attributed to the amount of segregated ice.

the freezing interface. The sensible heat loss was 0.62 cal/cm-sec in the case of maximum heaving (7 mm/day); higher values resulted in thermal conditions favoring sirloin-type freezing. The moisture content of frozen soil was found to be related to the heaving ratio, inasmuch as the amount of heaving is attributed to the amount of segregated ice.

the freezing interface. The sensible heat loss was 0.62 cal/cm-sec in the case of maximum heaving (7 mm/day); higher values resulted in thermal conditions favoring sirloin-type freezing. The moisture content of frozen soil was found to be related to the heaving ratio, inasmuch as the amount of heaving is attributed to the amount of segregated ice.

the freezing interface. The sensible heat loss was 0.62 cal/cm-sec in the case of maximum heaving (7 mm/day); higher values resulted in thermal conditions favoring sirloin-type freezing. The moisture content of frozen soil was found to be related to the heaving ratio, inasmuch as the amount of heaving is attributed to the amount of segregated ice.

CONTENTS

TABLES

ILLUSTRATIONS

SUMMARY

Laboratory studies on the effects of the soil-temperature regime on the type of ice segregation and the rate of frost heaving are described and analyzed quantitatively on the basis of thermodynamic and hydraulic theory, assuming that suction is created by ice formation.

The type of ice segregation is correlated with freezing line penetration as well as with frost-heaving rate. The ice filament layer or sirloin type of ice segregation, with high ice content, develops at low penetration rates and the concrete type at high penetration rates. The concrete type of freezing gives a lower heaving rate than the sirloin or ice-filament type.

The heaving rate $d\xi/dt$ decreases with increasing frost-penetration rate dx/dt according to the equation

$$d\xi/dt = A - B\, dX/dt$$

where the constants A and B are functions of the original dry density of the soil. For the ice-filament layer type of ice segregation, the heaving rate increases with sensible heat loss at the freezing interface up to a maximum value of heat loss, beyond which the freezing line drops and the type of freezing changes.

Moisture content of the frozen soil is related to the heaving ratio, inasmuch as the amount of frost heaving is attributed to the amount of segregated ice in the soil.

EXPERIMENTAL STUDY OF FROST HEAVING

by
Akira Higashi

INTRODUCTION

The development of railroads, highways, and airfields in the northern regions of the world has created an urgent need for information on the behavior of soil in cold climates. Frost heaving has long been known as a major destructive factor for structures whose foundations are subjected to low temperature environment. Many investigations have been conducted to determine means for preventing damage by frost heaving as well as to provide a clear understanding of the mechanics of this phenomenon.

Because so many factors influence frost heaving, it is difficult to clarify the frost-heaving mechanism. It is possible that some popular misconceptions about frost heaving result from unsuitable experimental test procedures. It is extremely important to simulate natural conditions while at the same time eliminating factors of minor importance.

The factors which influence frost heaving may be divided into two major categories; extrinsic, those which are outside of the soil but condition it, and intrinsic, those which belong to or are properties of the soil.

Intrinsic factors include moisture conditions, soil structures, density, physical and chemical composition, permeability, capillarity and thermal properties. The effects of some of these factors have been thoroughly investigated and the results of these investigations have been applied to practical construction.

Extrinsic factors include climate, the ground water level, and the surface conditions of the soil. In conjunction with the intrinsic factors, these establish thermal and hydraulic conditions in the soil which are favorable or unfavorable to frost heaving. In spite of the fact that these conditions determine the nature and extent of frost heaving, little work has been done to develop relationships between them and frost heaving.

The principal purpose of these experiments is to determine how the temperature regime in the soil affects the type of ice segregation and the rate of frost-heaving. In nature the main factor effecting a change in the soil temperature is the air temperature over the ground surface. The experiments were designed to simulate temperature changes over the ground surface. Temperature distribution in the soil was obtained by thermocouples embedded in the soil sample, which makes it possible to analyze the thermal regime in the soil using the heat balance equation. For this analysis, the thermal conductivity and the specific heat of the soil were measured, using apparatus especially designed for this purpose. The effects of permeability and porosity of the soil on the type of ice segregation were investigated experimentally by changing the dry density of the soil. The experimental results were explained quantitatively by combining thermodynamic theory and hydraulic theory, the latter theory being based on an assumption of a suction force originated by the existence of ice. The results show that the system adopted for the supply of water is a realistic way to simulate frost heaving under natural conditions.

SOIL MATERIAL AND EXPERIMENTAL METHODS

Soil

Bloomington silt obtained from a till deposit near the Fox River in northern Illinois was used. This is a brown, frost-susceptible subsoil. Though it is called a silt, its physical characteristics (Table I) show that the soil belongs to the group of "glacial clay".

Table I. Physical characteristics of the soil (all measured by ASTM standard methods).

Specific gravity	2.63	g/cm³
Liquid limit	31	%
Field moisture content	22	%
Plastic limit	14	%
Plasticity index	17	%
Shrinkage limit	12	%

It is classified as CL by the unified soil classification system. The particle size distribution curve is shown in Figure 1. The air-dried soil was sieved over a 1-mm screen and crushed to break up any lumps, therefore the soil does not include any particles larger than 1 mm in diameter.

As the relationship between the dry density and the saturation moisture content is employed in some later calculations, the porosity was calculated as a function of the unit dry density by

$$\frac{\gamma}{G} + n = 1. \qquad (1)$$

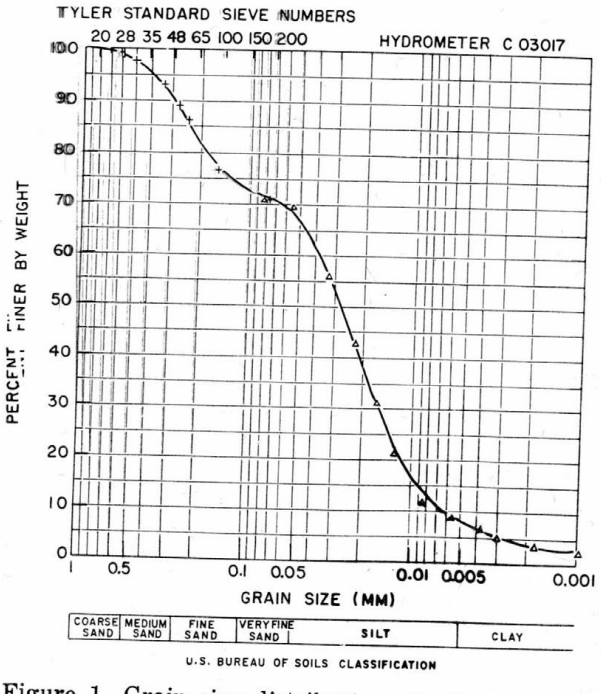

Figure 1. Grain size distribution of soil used for experiments.

where γ is unit dry density, G is the specific gravity, and n is the porosity. The saturation moisture content is defined by

$$w_s = \frac{n\gamma_w}{\gamma} \qquad (2)$$

where γ_w is the density of water. Results of calculations are shown in Figure 2.

Observed values of saturation moisture content in the soil sample, prepared as described later, are always lower than the values calculated from eq 2. The observed values are expressed as a broken line curve in Figure 2. This tendency is probably due to air bubbles among soil particles which cannot be easily displaced by the water.

Permeability was measured by a "falling head" test at various degrees of compaction (dry density). The results of the tests are shown in Figure 3. Permeability changes quite remarkably in the relatively narrow range of dry density with which we are concerned.

Freezing system

The insulated cabinet that held the samples while freezing was designed to permit simultaneous testing of four samples (see Fig. 4). This cabinet is a wooden box with insulated walls made of foamglass. The four samples are separated by foamglass bricks and are supported over a pan by a plate with four square openings. This pan serves as a source of water under the samples and contains a heating coil connected to a thermoregulator which maintains a constant water temperature.

This setup induces vertical heat flow inside the sample container. Some lateral heat losses were shown by the curve of vertical temperature distribution (Fig. 12). However, this did not disturb horizontal uniformity of temperature distribution.

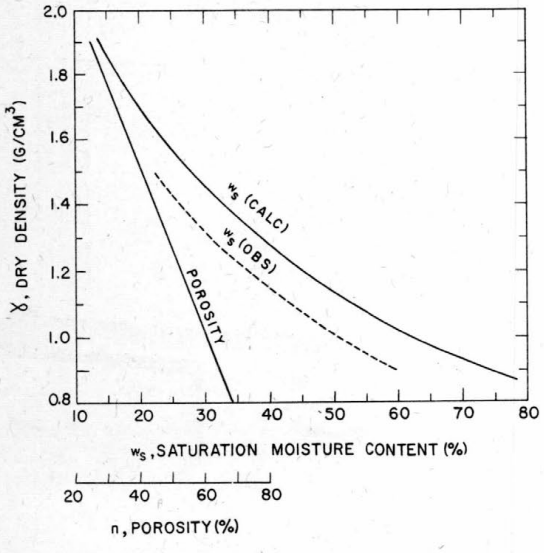

Figure 2. Porosity and saturation moisture content vs dry density of the soil.
n = % of volume of soil;
w_s = % of weight of dry soil.

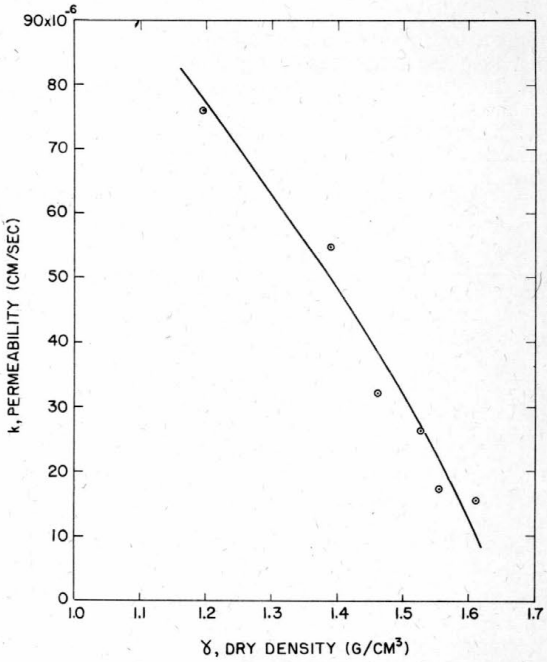

Figure 3. Permeability of the soil vs dry density.

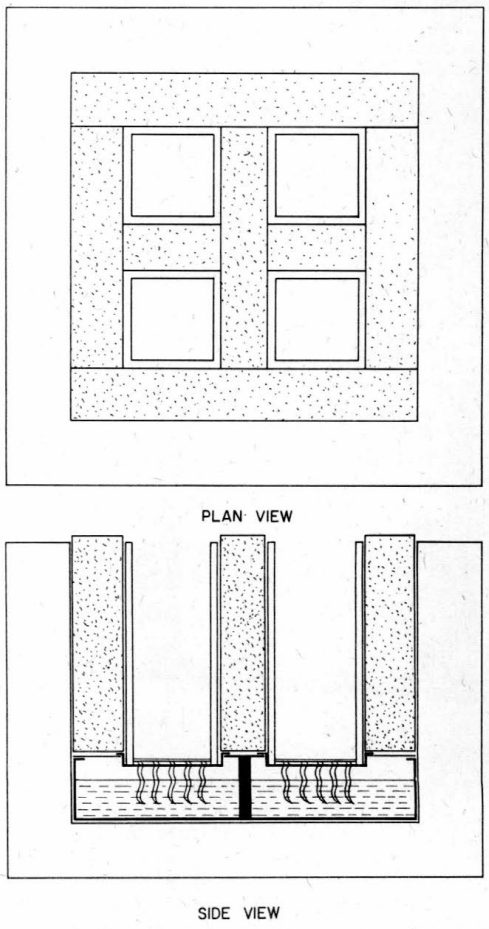

Figure 4. Design of the freezing cabinet.

That a uniformly horizontal lowering of the freezing line is achieved is clearly demonstrated by the horizontally parallel formation of ice layers in the soil sample.

The containers for the sample are made of wood and have a square cross section (8 x 8 cm square and 21 cm high). The inside walls are coated with silicone grease to eliminate friction between the soil sample and the walls during heaving. The bottom of each container is of perforated copper through which wicks are hung into the water below. The use of wicks to accurately simulate natural hydraulic conditions is explained in detail in the discussion.

The cabinet is placed inside a box where the air temperature can be kept constant to ± 0.5C by a thermoregulator connected to heat tapes. By placing this box in a cold room at -20C, the air temperature over the sample can be regulated in the range $+15$C to -20C.

The samples were prepared in duplicate. One sample from each pair was instrumented with thermocouples to provide a record of the changing temperature distribution. The final moisture distribution was also obtained from this sample. Specimens from the other samples were used to determine thermal diffusivity for corresponding types of ice segregation.

Thermocouples and heave-measuring apparatus

Six thermocouples were embedded in one sample of each pair at various depths and one was placed directly on the soil surface. Thermocouples were placed in grooves cut along two corners of the container and were bent horizontally toward the center of the container at each desired depth. As this was done before the container was filled, the compaction of the soil altered the depth of the thermocouples.

In addition to the initial displacement, tips of the thermocouples moved upward during freezing. This movement must be parallel to the heaving at the surface since the thermocouple that moves is in the frozen part of the sample. The final position of each thermocouple was measured upon completion of the test. If the heaving vs time curve is known, we can obtain the movement-time curve

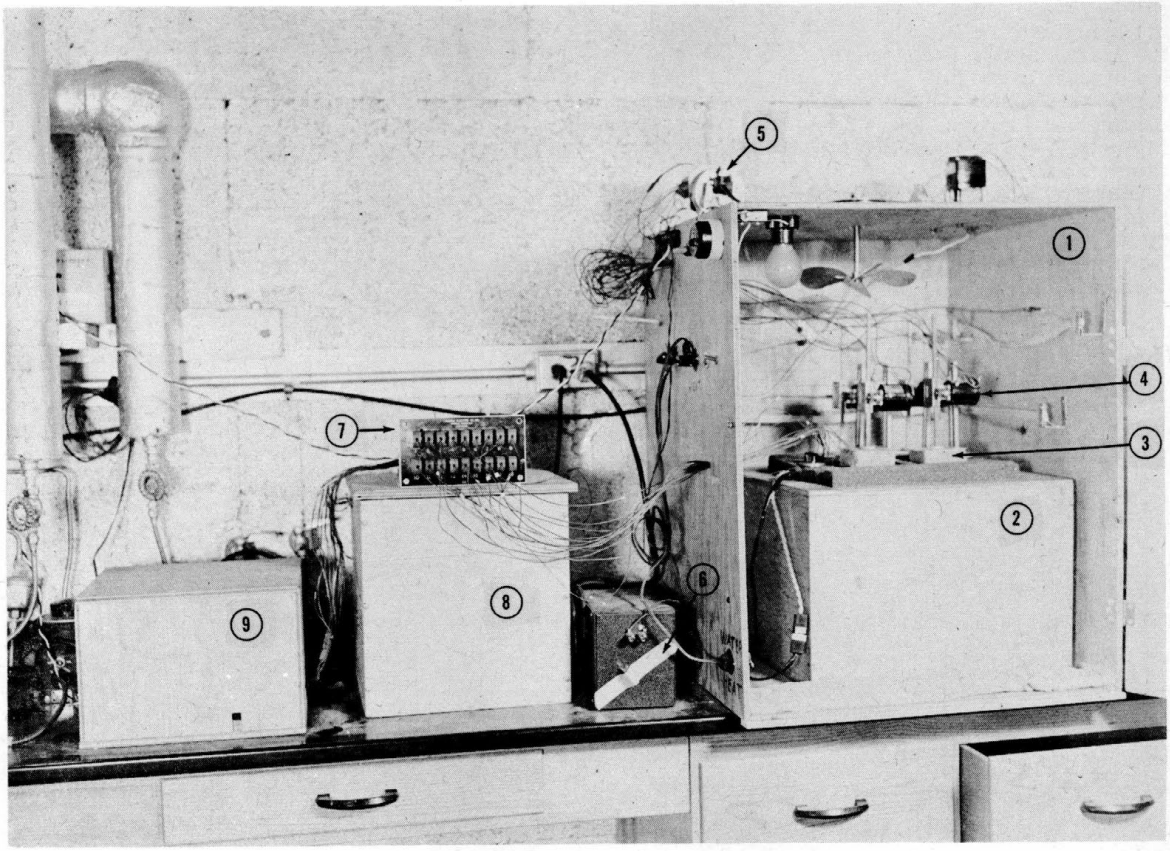

Figure 5. General view of the test equipment.
(1) Test sample cabinet (front door open). (2) Freezing cabinet (3) Soil Samples.
(4) Potentiometers for measuring frost heave. (5) Timing switch for potentiometers.
(6) Converter stabilizer for potentiometer circuit. (7) Thermocouple connecting panel.
(8) Ice bath for thermocouples. (9) Timing switch for thermocouples.

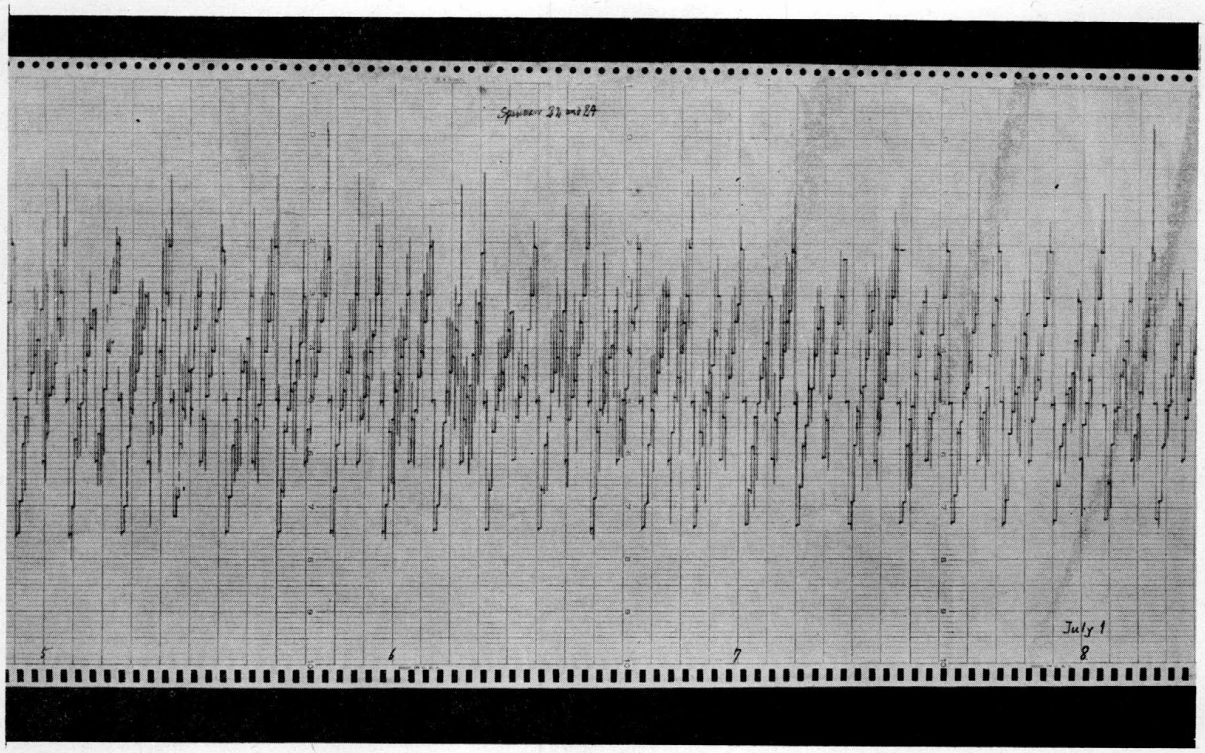

(a) Temperature

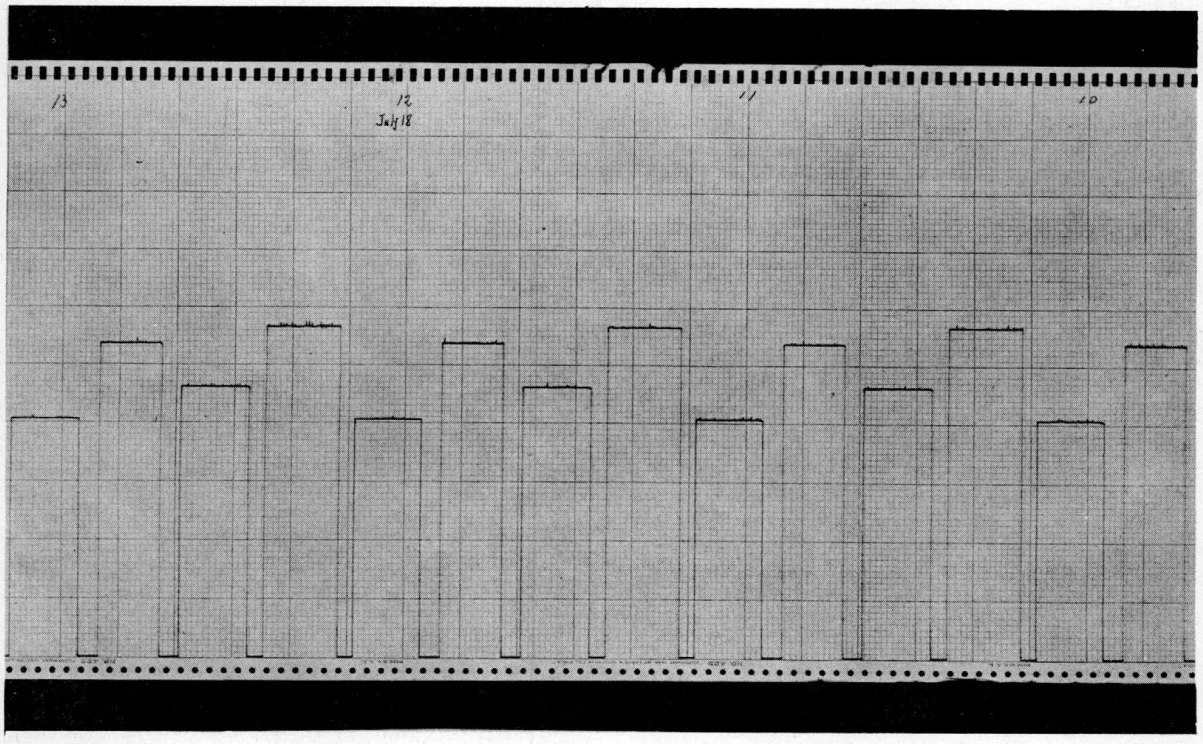

(b) Frost heaving

Figure 6. Sample chart records of temperature and frost heaving

of each thermocouple by drawing a curve parallel to the heaving curve. The depth of each thermocouple at the time when it indicated freezing temperature of the soil moisture must be the initial depth of the thermocouple.

By quick freezing of a sample prepared in this manner, it is possible to measure the displacement due to compaction, since the amount of heave is negligible in this case. Values obtained by this method checked closely with values obtained by the indirect method.

Eighteen thermocouples, including two for measuring the air temperature, one for the water temperature in the pan, and another for the ice bath in addition to the twelve placed in the soil samples and the two on the surfaces, were attached to a thermocouple connecting board, which made it easy to connect or disconnect the thermocouples and the measuring circuit. Thermocouple wires from the connecting board were lead to an ice bath maintained at OC and the lead wires from the reference junctions were connected to a rotary selector switch. This switch permits the cyclic reading of temperature indicated by each thermocouple on the chart of a one-pen recorder. The time interval of contact for each thermocouple is adjusted to about 30 sec by means of a cam connected to a timing motor. A sample record of temperature is shown in Figure 6a.

Heaving at the surface of each sample was measured by a potentiometer. The vertical heaving motion was transferred into a rotary motion of the potentiometer shaft by a rod attached to a rack and pinion mechanism. The potentiometers were kept at a constant height by stands fastened to the edges of the containers. Rotation of the potentiometer shaft caused a change of resistance between two terminals which were connected to the input of the recorder. This potentiometer makes the output voltage proportional to the amount of heaving. The apparatus and the electric circuit with the timing switch are shown in Figure 7a,b. The timing switch was adjusted to record heaving for each potentiometer for about 15 min, followed by a 2-min break, as shown on Figure 6b. Voltage was so adjusted that a 1-in. deflection of the pen on the chart corresponds to a heave of 1.0 cm. The amount of heave was

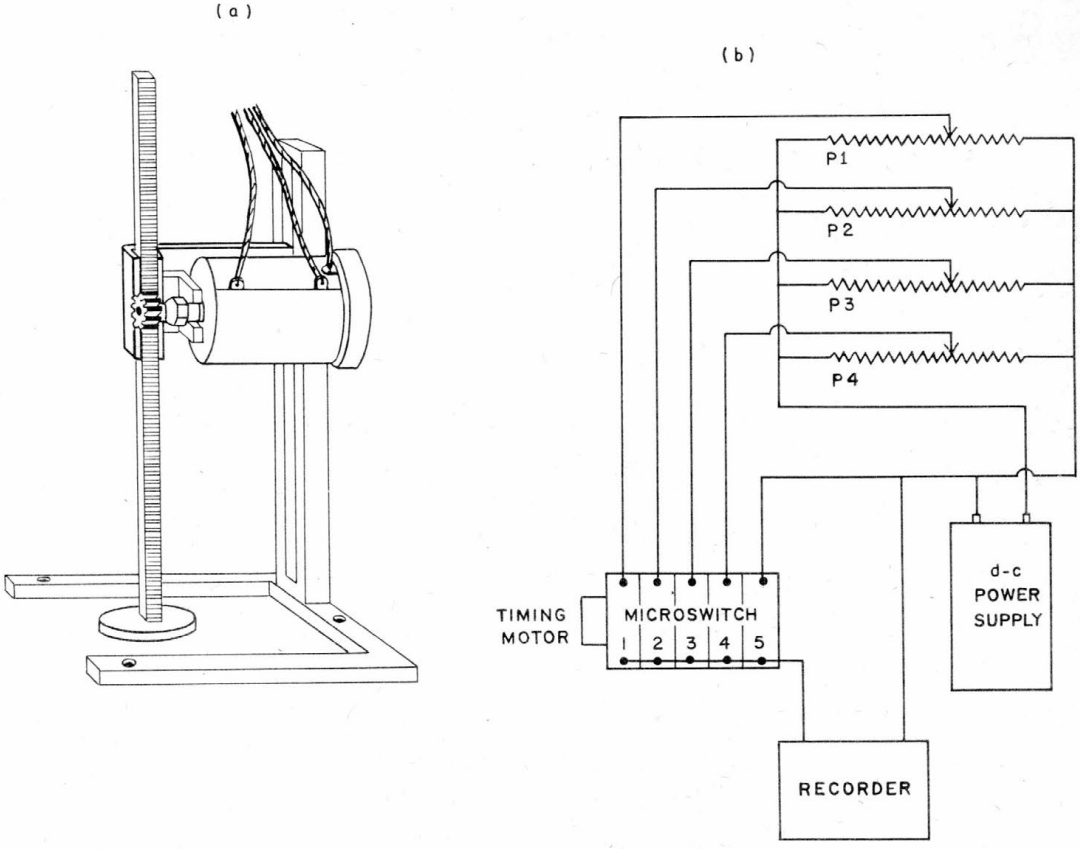

Figure 7. Apparatus for measuring frost heaving

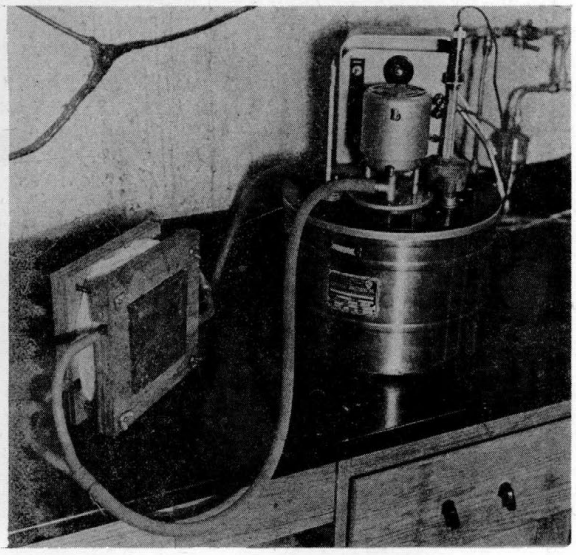

Figure 8. Apparatus for measuring thermal diffusivity of the soil.

easily obtained with an accuracy of 0.1 mm. One sample of a heave record is shown in Figure 6b. A general view of the apparatus is shown in Figure 5.

Apparatus for measurement of thermal diffusivity

The apparatus for measuring thermal diffusivity (Fig. 8) consisted of two copper plates between which a flat specimen is sandwiched. A flat tank was attached to the outside of each plate and a cooling liquid circulated through it by a pump of a constant temperature bath kept the plates at a constant temperature.

After inserting a soil specimen between the plates and insulating the sides of the specimen, the apparatus was left at a constant temperature in a cold room for a few hours to reach thermal equilibrium. Then the cooling (or warming) liquid at a constant temperature was circulated through the tanks and the temperature of both plates changed suddenly to another constant temperature.

The temperature at the center of the specimen gradually rose or fell and finally reached the same temperature as the plates. According to the theory of heat conduction, the temperature change at the center of a specimen of thickness a is

$$\theta - \theta_0 = \frac{4(\theta_1 - \theta_0)}{\pi} \exp\left(-\frac{\pi^2}{a^2}\alpha t\right) \qquad (3)$$

where

θ = temperature at the center at time t
θ_1 = initial temperature of the specimen
θ_0 = final temperature of the specimen
t = time measured from the moment of surface temperature change
α = thermal diffusivity of the soil

Temperature at the center of the specimen was measured by very thin thermocouples (BS # 36) buried carefully in a hole drilled to the center. This temperature was recorded on a time temperature curve and α was calculated from eq 3.

Heat-transfer calorimeter

To measure the specific heat of the soil, a heat-transfer calorimeter was used. The original design of this type of calorimeter (Yosida and Wakiya, 1950) was modified by the present author (Higashi and Murao, 1954) to allow measurements to be made electrically. As these papers are available only in Japanese the details of this calorimeter are described here.

The principle behind this measurement is entirely different from the "method of mixture" used in the ordinary calorimeter. The calorimeter is a double-walled metal cylinder (Fig. 9a) with narrow clearance between the two walls filled with silicone oil. The calorimeter is kept in a constant temperature bath. The sample is heated to a definite temperature above that of the calorimeter and then placed in the cylinder. Heat from the sample will then flow through the double wall and be transferred into the liquid in the bath.

The principle of this calorimeter requires measurement of the total heat transferred and a knowledge of the initial heat content of the sample. This is a very convenient method for materials of low heat conductivity such as soils, because it is not necessary to keep heat inside the calorimeter, as with the method of mixture. In this latter method, when the time of heat exchange is prolonged, heat dissipation from the calorimeter is apt to cause large error in measurement.

As the thermal conductivity of the metal wall is higher than that of the oil in the space between the two cylinders, the main part of the temperature gradient between the inside and the outside of the calorimeter is in the oil. Hence the rate of heat flow through the oil must be proportional to the temperature difference between the two walls, that is to say

$$\frac{d\theta}{dt} = \frac{2\pi K(u_1 - u_2)}{\ln r_2 - r_1}\,\ell. \qquad (4)$$

In this equation, $d\theta/dt$ is the heat flow through the walls per unit time, u_1 and u_2 are the temperatures of inside and outside walls respectively, r_1 and r_2 are the distances of the inside and outside of the oil layer from the center of the cylinder, K is the thermal conductivity of the oil, and ℓ is the length of the cylinder. As the quantities K, r, and ℓ are constant for the calorimeter, eq 4 is rewritten as

$$\frac{d\theta}{dt} = C(u_1 - u_2) = C\Delta u \qquad (5)$$

where Δu is the temperature difference between the two cylinders and C is a constant.

Integrating this equation, we obtain the total heat Q transferred from the material to the outside of the calorimeter as

$$Q = \int_0^T \Delta u \, dt. \qquad (6)$$

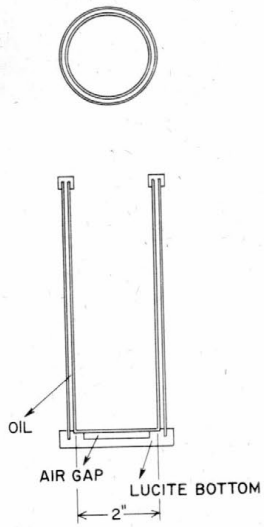

(a) Design

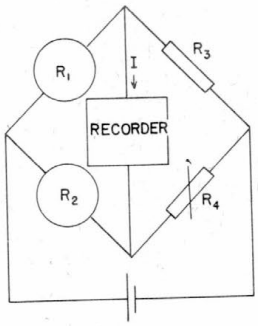

(b) Electrical circuit

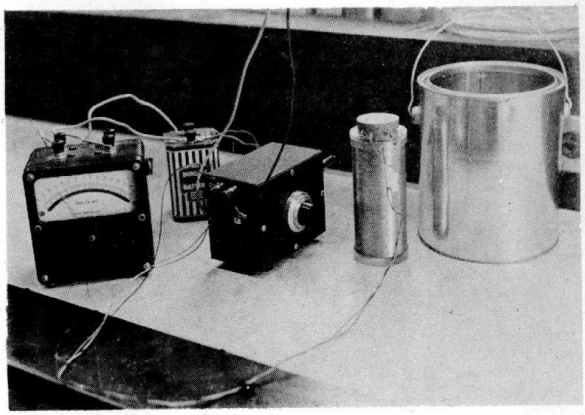

(c) Apparatus

Left to right: voltmeter; dry cell, 3v; resistances in Wheatstone bridge with one variable resistance; double-wall cylinder for calorimeter; container for calorimeter.

Figure 9. Heat-transfer calorimeter

T is the time at which the system reaches equilibrium, measured from the moment when the sample is placed in the calorimeter. Integration of Δu is obtained by an electrical method as follows.

Thin copper wires (BS # 40, enamel covered) are wound around the outside of each cylinder. Winding on the outer cylinder is visible in Figure 9c. Each wire has a resistance of about 40 ohms. Connecting these wires with two other resistances in the form of a Wheatstone bridge as is shown in Figure 9b, the temperature difference between the two cylinders is measured. The bridge is balanced when the calorimeter is empty and its temperature is in equilibrium with the liquid in a constant temperature bath. When a warmer materal is placed in the calorimeter, the inner cylinder becomes warmer than the outer one and disturbs the balance of the bridge circuit. In that case, the current flowing through the recorder is proportional to Δu. If we designate the current by I, eq 6 is written as

$$Q = C' \int_0^T I \, dt. \qquad (7)$$

This equation means that the integration of the current is proportional to the heat transferred. The integration is easily obtained as an area enclosed by a time-current curve and time coordinate on a chart from the recorder. If each constant for the calorimeter and the Wheatstone bridge circuit is known, the proportionality constant C′ can be determined by calculation. Actually, to avoid the complexity of this calculation, C′ was determined by calibration, using different materials of known specific heat.

Once the transferred heat Q for a soil placed in the calorimeter is known, the specific heat s of the soil sample is obtained by

$$s(u_i - u_f)m = Q$$

where u_i and u_f are the initial and final temperature of the soil put in the calorimeter and m is the mass of the soil.

One possible source of error is the assumption that the heat from the material inside the calorimeter is transferred to the bath only through its side walls. Heat transfer through the bottom is kept quite small by supporting the inner cylinder on the Lucite bottom with an air gap between the bottom of the cylinder and the Lucite (Fig. 9a). The top of the cylinder is insulated with a thick cork stopper after the material is inserted. In addition, the cylinders were so made as to have relatively small end areas as compared with the sidewall area. The ratio of end areas to the sidewall area was about 1/6 and the ratio of heat flow is believed to be less than 1/30, considering the difference of thermal conductivity among oil, cork, and air.

Though it is not necessary to maintain a constant temperature for the liquid in the bath, a large can filled with silicone oil was used in the actual experiments to minimize temperature changes of the outer cylinder.

EXPERIMENTAL PROCEDURES AND RESULTS

General procedures

After setting thermocouples in the two soil containers, as described in the preceding section, and measuring the depth of each, all four containers were filled with dry soil. Various dry densities (degree of compaction) ranging from 1.2 to 1.6

g/cm³ (75-100 lb/ft³) were obtained by varying the number of times each container was struck against a table top.

Filled containers were placed on the water pan and allowed to gain moisture under capillary action. After a few days the soils attained a stable condition and the moisture content was uniform throughout the specimen. Homogeneity of the dry density and of the moisture content in the soil sample was ascertained as follows. Two soil samples with dry densities of 1.3 and 1.4 g/cm³, prepared as described above, were quickly frozen at a temperature of —35C. As no moisture migration could have occurred in such a quick freezing process, the moisture content distribution and the dry density must have remained unchanged. The moisture contents and dry densities were determined for each 2-cm layer of each sample. It was easy to slice the frozen samples layer by layer and prepare cubes of definite dimensions for volume measurements. Distributions of dry density and moisture content with depth (Fig. 10) show that both are quite uniform except at the very top of the sample.

Four soil sample containers were placed in the insulated cabinet, the cabinet was placed in the temperature box, and the thermocouple wires were attached to the connecting panel. The potentiometers were fixed on each container by their supporting frames and their heights were adjusted to register zero heave on a recording chart.

Temperature in the box (air temperature) was kept above 0C for a while and then decreased in steps to below 0C. Recording of temperature and heaving began when the air temperature reached 0C. Generally, the air temperature was kept constant for a few days and then lowered to another constant value. The temperature was easily changed by adjusting the thermoregulator of the temperature box and the desired value was attained within one hour. The magnitude of a particular temperature drop was determined by the type of freezing desired in the succeeding step. Generally, one test series was continued for about 2 weeks.

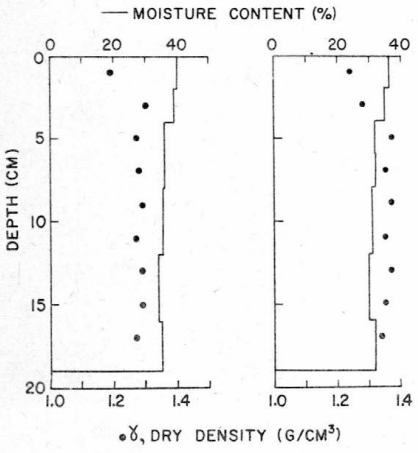

Figure 10. Distribution of moisture content (line) and dry density (dots) through the soil sample before freezing (blank test).

One example of the temperature changes during an experiment is shown in Figure 11. Corresponding soil temperatures at various depths are also shown. These temperature-time curves were obtained by plotting the individual temperature readings from the recorder chart (see Fig. 6a). The number on each curve refers to the thermocouple embedded in the soil.

When freezing had reached a certain depth, as determined by the temperature distribution in the soil, the experiment was halted and the sample container was removed from the cabinet. One side of each container was removed and the clearly visible freezing boundary of each sample was marked. Then, the samples were completely frozen at —35C without being returned to the cabinet, to prevent any further moisture migration.

The frozen samples containing thermocouples were cut in half along a vertical plane to expose the thermocouple tips. Distances between thermocouples were measured and the section was photographed. The half of the cut sample which did not contain thermocouples was used to measure the moisture content distribution. This was done by slicing the sample horizontally into small specimens 1 to 2 cm thick. These specimens were cut into cubes by smoothing the surfaces with a sanding-machine. This cube form made it possible to measure the volume of the specimen for the determination of dry density. After being weighed in the cold room the specimens were dried in an oven at 100C.

Soil temperature profile and penetration of the freezing line

The temperature profile in the soil at any time is obtainable from the temperature-time curves (e.g. Fig. 11), if the depth of each thermocouples is known exactly. As stated in the previous section, this depth changes during the compaction and saturation processes. As freezing advances in the soil, a thermocouple in the frozen part is raised by the heaving of the soil below. Thus, the vertical movement of a thermocouple is equal to the amount of frost heave that occurs after the temperature indicated by this thermocouple reaches the freezing point.

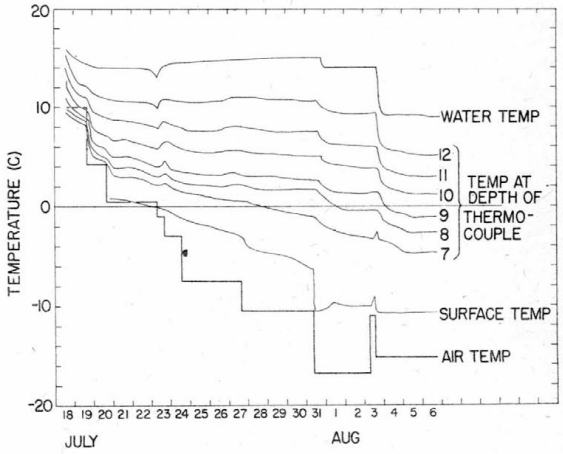

Figure 11. Temperature-time curve, sample 7. For depth of numbered thermocouples, see Fig. 13.

The freezing point of the soil moisture was depressed about 0.5C. This was verified by the fact that the real freezing boundary observed at the end of an experiment always lay at the −0.5C depth, not at the 0C depth. The dates on which each thermocouple reached the freezing point were easily determined from the temperature-time curves. For example (Fig. 11), in sample 7, thermocouple 7 reached −0.5C in the afternoon of 29 July and No. 8 on 3 August.

Paths of the thermocouples were obtained by tracing back parallel to the frost heaving curves from the final position of each thermocouple to the date on which the freezing point was reached. This process is illustrated on Figure 13. Frost heaving recorded for sample 7 was transferred to this figure as a continuous curve. The depth shown for thermocouple 7 on 29 July represents the original depth of the thermocouple before freezing. It is clearly seen that the top 3.2-cm layer expanded by 1.9 cm during the period 24 July to 29 July.

Using the depths obtained from these curves and the temperature-time curves as on Figure 11, temperature profiles in the soil during freezing can be drawn. Two examples are shown in Figure 12. The temperature profile is concave upwards in the unfrozen part and concave downwards in the frozen part. It is evident from the theory of heat conduction that the curve in the frozen part is characteristic of the temperature profile in the transition stage of freezing process. The gradient in the unfrozen part may be attributed to heat loss to the side of the containers. Temperature gradients in the layers near the freezing line, which are needed to calculate the thermal regime in the soil were determined as the tangents to these curves at about 1 cm above and below the freezing line. Depth of the freezing boundary was taken as the depth of −0.5C temperature. Penetration of the freezing boundary was obtained by plotting this depth every day or sometimes every 12 hours (see Fig. 13).

Types of ice segregation and their relation to frost heaving

The ice segregation was studied with the naked eye and with the aid of photographs of the cut sample. The types of ice segregation are classified as follows (1) ice filament layer, (2) sirloin-type freezing, and (3) concrete-type freezing. This nomenclature was developed by the present author based on a work by Nakaya and Magono (1940; 1942). To illustrate the classification, the photograph of sample 22 is reproduced in Figure 14.

The ice filament layer (designated by the letter "F" in Fig. 14) is composed of bundles of numerous ice filaments of minute crystals. Though it looks like a pure ice plate in the soil, it always contains air bubbles, which are generally elongated in the vertical direction and give an appearance of columnar structure to the ice. A thin horizontal cross section of the ice layer F_2 was inspected under the polarizing microscope. Figure 15 is a photomicrograph taken under crossed polaroids. The ice layer was composed of minute crystals of about 1 mm in diameter with random orientation. Black shadows in the picture are soil particles and the circular semi-transparent shadows are the air bubbles entrained in the ice.

Sirloin-type freezing (S in Fig. 14) is so named because the dispersion of innumerable thin ice layers in the frozen soil given it an appearance similar to a piece of sirloin beef. The particular appearance is determined by the amount of segregated ice. This can be seen by comparing the specimen's appearance with the corresponding moisture content distribution shown to the right.

The concrete type of freezing (C) does not show any degree of ice segregation and gives the appearance of a concrete matrix.

In accordance with preliminary classification by the Frost Effects Laboratory (1952), concrete-type freezing corresponds to classification code NW. Both sirloin type and ice filament layer freezing may be grouped under the code IS and differentiated by additional description of ice lenses and

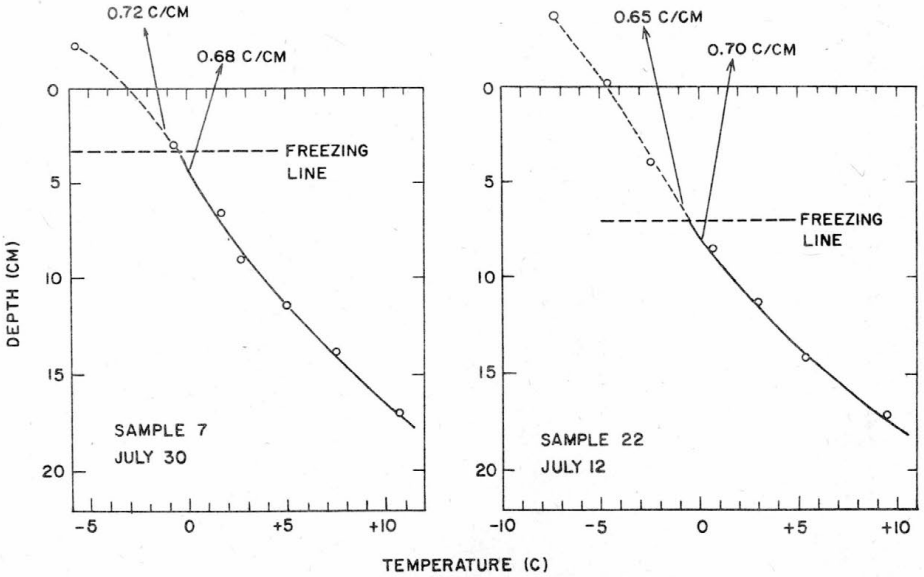

Figure 12. Typical soil temperature gradients.

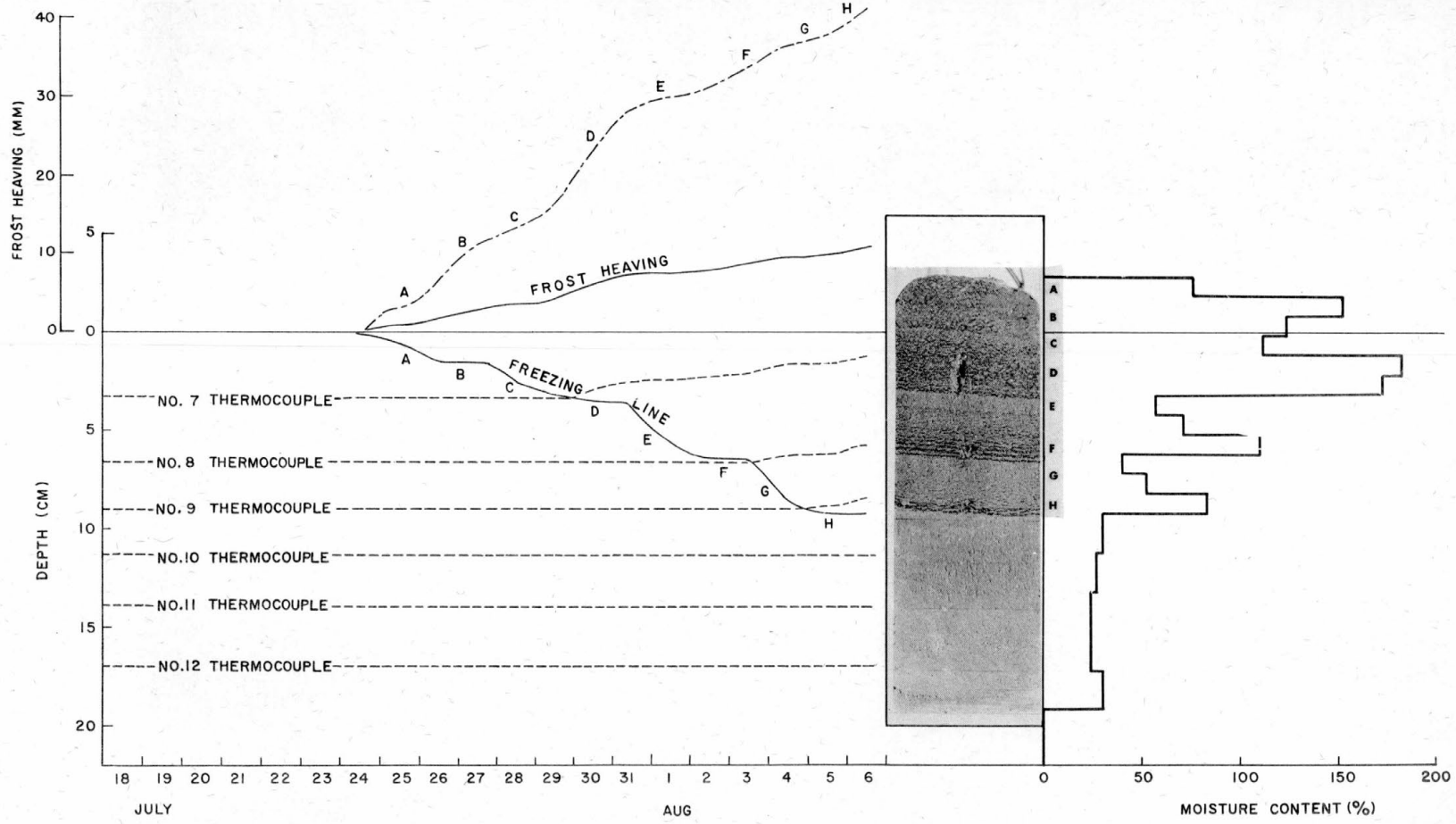

Figure 13. Frost heaving, freezing line penetration, and paths of thermocouples during soil freezing. Dot-dash line shows the frost heaving curve at a 4 times larger scale (in mm) for detail. Moisture content of the soil after freezing and corresponding types of ice segregation are shown to the right.

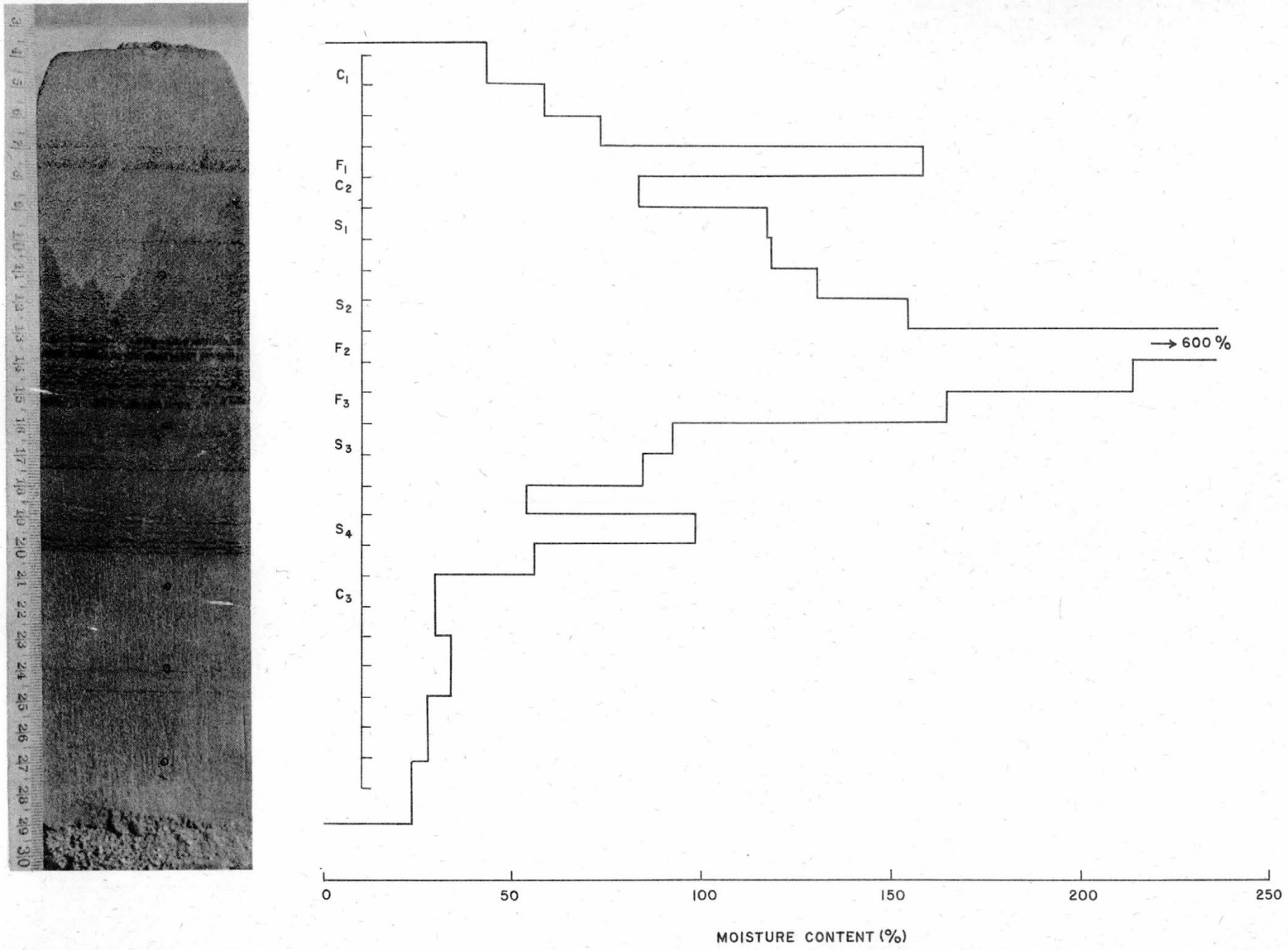

Figure 14. Types of ice segregation and corresponding moisture content, sample 22.

ice segregation. The correlation between the two systems is considered to be approximate and comparisons made would not be precise.

The occurrence of these freezing types is related to the rate of frost heaving and to the rate of penetration of the freezing boundary. To demonstrate these correlations, reference is made to Figure 13. Following any partciular thermocouple path back to where it intercepts the freezing line gives the original depth of its corresponding frozen soil layer. Directly above this point, on the frost heave curve, the rate of heaving can be determined. Each layer designated A, B, - - -,H on the photograph corresponds to the section of the freezing line with the same designation. From this, we can clearly see that the ice filament layer or sirloin type, with high ice content, occurred when the penetration rate was very slow while the concrete type developed when the penetration rate was rapid. It is also evident that the concrete-type freezing gave a lower heaving rate than the sirloin type or the ice filament layer type.

These correlations provide another correlation between the frost heaving rate and the freezing line penetration rate. This will be treated quantitatively in the next two subsections.

Moisture content of the frozen soil, heaving ratio and type of ice segregation

Examples of moisture content measurements are shown on Figures 13 and 14. These figures give a rough idea of the relationship between types of ice segregation and moisture content of the frozen soil. Frozen soil classed as concrete type has a moisture content less than about 40%. The sirloin type has a wide range of contents above 40%. As the ice filaments layer is defined as a bundle of ice filaments or minute crystals, the moisture content of a pure specimen of this type would be infinite. But the ice filaments layer often contains a small quantity of soil. If it contains 10% of soil by volume the moisture content is about 600%. Therefore, the boundary moisture content between the sirloin type and ice filaments layer is over several hundred percent. For example layer F_2 (Fig. 14) is cut to include only the ice filament layer and the moisture content exceeds 600%. Layers F_1 and F_3 take in more than the ice filament layer, and their moisture contents are comparatively small, though more than for the sirloin types (S_1, S_2, S_3, S_4).

If frost heaving is attributed to ice segregation in the frozen soil, the moisture content of the frozen soil layer should be related to the heaving ratio. This is the ratio of the amount of frost heaving to the depth of freezing line penetration for the time during which the frozen layer was formed. The relationship is represented as follows:

$$\text{Heaving ratio} \quad \frac{\Delta\xi/\Delta t}{\Delta X/\Delta t}$$

$$= \frac{\text{height of segregated ice}}{\text{depth of freezing line penetration}}$$

$$= \frac{\gamma V(w-w_s)v_i}{V}$$

$$= \frac{(\text{mass of excess water})\ (\text{spec. vol. of ice})}{\text{volume of the water saturated soil}}$$

$$= \gamma(w-w_s)v_i . \qquad (8)$$

$\Delta\xi/\Delta t$ and $\Delta X/\Delta t$ can be obtained at any time as a tangent to the frost heaving curve and the freezing line penetration curve respectively. Using a method similar to that for determining thermocouple depths, we can trace the original depth of any layer or the date on which the layer froze. Taking $\Delta\xi/\Delta t$ and $\Delta X/\Delta t$ as stated above, we can get $\Delta\xi/\Delta X$ vs $\underline{w}$ relations for each section for which moisture content was determined.

As the sections for the moisture content determination were 1 cm thick each, some of them extended over two layers of different freezing types or, in some instances, segments of the time-temp curve are too short to have had an appreciable effect on a specimen of this thickness. Omitting such cases, relationships between $\Delta\xi/\Delta X$ and $\underline{w}$ as shown in the Table II were obtained. Data for sample 7 can be checked in Figure 13. These relationships with data from other samples are graphed on Figure 16.

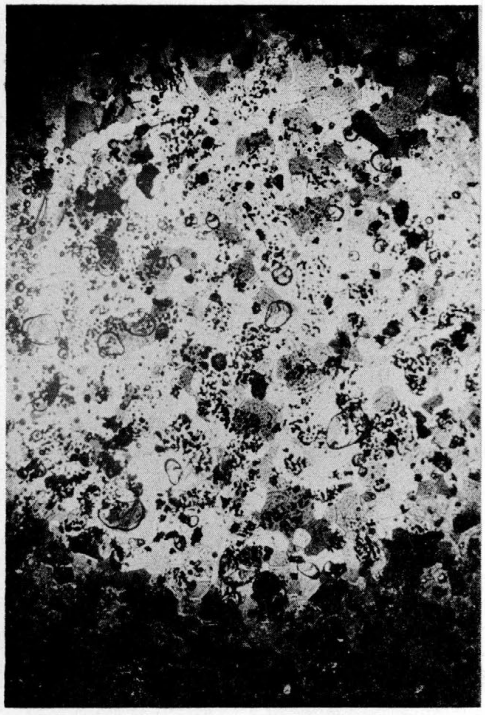

Figure 15. Photomicrograph of a thin section of an ice filament layer, F_2, from sample 22. Taken under crossed polaroids.

Table II. $\Delta\xi/\Delta X$ vs $\underline{w}$ relationships in the frozen soil.

Sample No.	Date of freezing	$\Delta\xi/\Delta t$ (mm/day)	$\Delta X/\Delta t$ (mm/day)	$\Delta\xi/\Delta X$	w (%)
3	9-10 July	4.0	11.0	0.36	60
"	11 "	4.0	13.0	0.31	53
"	12-13 "	8.0	2.0	4.00	390
"	16-17 "	9.0	5.0	1.80	175
5	24-25 "	4.0	7.0	0.54	61
"	28 "	5.0	5.0	1.00	112
"	1- 2 Aug.	1.0	3.0	0.33	49
7	25-26 July	3.0	7.5	0.40	75
"	29-30 "	6.5	3.0	2.16	178
"	31- 1 Aug.	2.0	19.0	0.11	56
"	3- 4 Aug.	3.0	21.0	0.14	40
22	28-29 June	2.0	27.0	0.07	59
"	13 Aug.	6.0	3.0	2.00	214
"	15-16 "	2.0	18.0	0.11	54
24	27-28 July	2.5	11.0	0.23	52
"	30 July	2.0	10.0	0.20	42
"	13-14 Aug.	2.5	4.0	0.62	73
"	15-16 Aug.	1.5	9.0	0.17	41

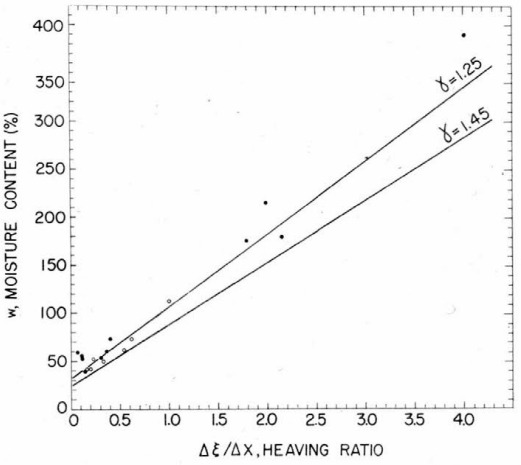

Figure 16. Moisture content of frozen soil vs heaving ratio.
Solid dots = original dry density 1.2-1.3 g/cm³ (samples 3, 7, 22)
Circles = original dry density 1.4-1.5 g/cm³ (samples 5, 24)

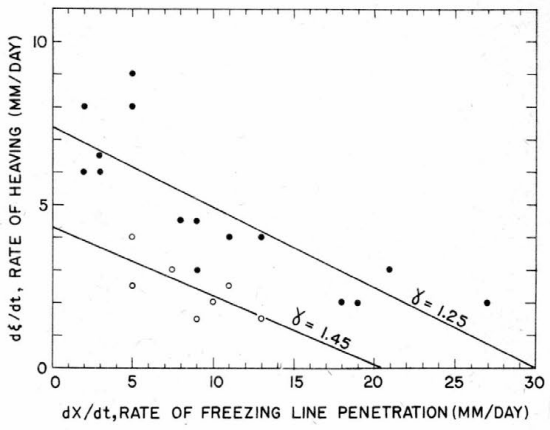

Figure 17. Rate of heaving vs rate of freezing line penetration
Solid dots = original dry density 1.2-1.3 g/cm³
Circles = original dry density 1.4-1.5 g/cm³

Eq 8 gives two lines on the figure corresponding to two different dry densities. The slope of each line is given by $\gamma\underline{v}_i$ and the ordinate for $\Delta\xi/\Delta X=0$ is given by the corresponding $\underline{w}_s$. This $\underline{w}_s$ is obtained from the experimental values shown on Figure 2. Coincidence of the points and lines is satisfactory and establishes the fact that frost heaving is caused by ice segregation in the frozen soil.

Relationship between heaving rate and the rate of freezing line penetration

As stated previously the heaving rate varies with the type of ice segregation, which varies with the rate of freezing line penetration. This means that the heaving rate is related to the rate of freezing line penetration. From Figure 13, it can be seen that the higher the rate of freezing line penetration, the lower the heaving rate. This relationship was checked quantitatively using data from several samples of different original dry densities.

Using those parts of the freezing line penetration curves that show a constant slope for one day or more, the rate of penetration was determined. The heaving rate on the corresponding date was determined from the tangent to the heaving curve. For example, on 25 and 26 July on Figure 13 the penetration rate dX/dt is 9.0 mm/day and the heaving rate $d\xi/dt$ is 4.5 mm/day. Correlations obtained from the curves of several experiments are tabulated in Table III and are plotted in Figure 17.

Table III. $d\xi/dt$ vs dX/dt relations.

Sample No.	Date	$d\xi/dt$ (mm/day)	dX/dt (mm/day)
3	9-10 July	4.0	11.0
"	11 "	4.0	13.0
"	12-13 "	8.0	2.0
"	16-17 "	9.0	5.0
"	18 "	6.0	2.0
5	24-25 "	3.0	7.5
"	28 "	4.0	5.0
"	3- 4 Aug.	1.5	13.0
7	25-26 July	4.5	9.0
"	27-28 "	3.0	9.0
"	29-30 "	6.5	3.0
"	31- 1 Aug	2.0	19.0
"	3- 4 "	3.0	21.0
22	28-29 July	2.0	27.0
"	13 Aug.	6.0	3.0
"	14-15 Aug.	8.0	5.0
"	15-16 "	2.0	18.0
"	16-17 "	4.5	8.0
24	27-28 July	2.5	11.0
"	30 "	2.0	10.0
"	13-14 Aug.	2.5	5.0
"	15-16 "	1.5	9.0

Any group of these plots seems to be represented by the empirical formula

$$\frac{d\xi}{dt} = A - B\frac{dX}{dt} \qquad (9)$$

where A and B are constants which seem to depend on the original dry density of the soil sample. Values of A and B, determined by the method of least squares from the data of Table III, are tabulated in Table IV.

Table IV. Values of constants A and B in eq 9.

Original dry density (g/cm^3)	A (mm/day)	B
1.25	7.4	0.25
1.45	4.2	0.21

An inspection of Figure 17 indicates that parabolic curves might best fit the plotted data. However, the fact that the rate of heaving becomes zero when the rate of freezing line penetration exceeds a certain value required the adoption of an equation with a linear regression of the type above. The significance of this equation from the hydraulic point of view will be given in the discussion.

Thermal conductivity of the soil

Results of the thermal diffusivity measurements are tabulated in Table V. Specimens 7 and 8 were made by freezing unsaturated soils and no. 9 was a sample of dry soil. The other specimens were prepared by cutting suitable frozen layers from the duplicate frozen samples. Though the effect of dry density cannot be neglected in the range of unsaturated moisture content, it was not considered here because all samples treated later fell within the over-saturated moisture range. A measurement for commercial ice is included. The result coincides well with the accepted value for ice, 11.2×10^{-3} cm^2/sec.

The relationship between the thermal diffusivity, α, and the moisture content, w, of the frozen soil is shown in Figure 18. Thermal diffusivity increases with the moisture content. The curve is

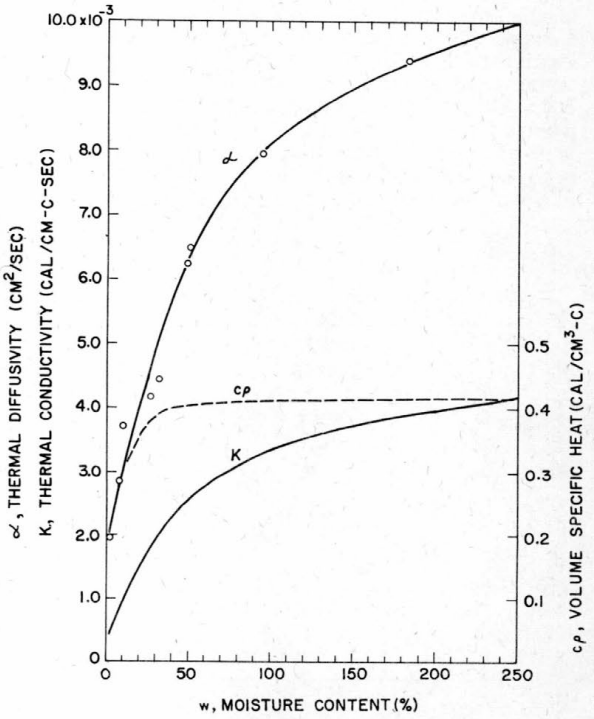

Figure 18. Thermal properties of frozen soil in relation to moisture content.

Table V. Thermal diffusivity of the frozen soil.

Specimen	Sample no. and depth from which the specimen was taken	Moisture content (%)	Thermal diffusivity (cm^2/sec)
1	No. 6 8 - 11 cm	51	6.48×10^{-3}
2	No. 6 5 - 8 cm	183	9.40
3	No. 6 below freezing depth	27	4.17
4	No. 6 top of the sample	95	7.94
5	No. 20 2 - 5 cm	49	6.24
6	No. 20 below freezing depth	32	4.43
7	Unsaturated	10	3.72
8	Unsaturated	8	2.85
9	Air dried soil	2	1.95
	Commercial ice		10.74

quite steep at low moisture content and then gradually become asymptotic to the value of ice.

Thermal diffusivity of the unfrozen soil was measured only in the saturated condition. The mean value of several measurements was 4.02 x 10^{-3} cm^2/sec.

Specific heat of the soil was measured with the heat-transfer calorimeter. The calibration of the calorimeter was carried out using aluminum rods and different weights of NaCl powder. Calibration below and above 0C coincide well (Fig. 19). The ordinate on the calibration curve represents recording chart areas for a chart speed of 1/10 inch per minute. This speed was kept constant throughout the measurements. Scattering of the points from the calibration curve (straight line) on Figure 19 shows that the standard error of estimation by this curve is about 3%.

A sample chart of an actual measurement is shown in Figure 20. This corresponds to test 6 in Table VI, which shows all data of the measurements and calculations. All the measurements were carried out with air-dried soil. Correction for the small quantity of water was required for calculating the specific heat of the soil. The relationship between the specific heat of the dry soil and temperature is shown in Figure 21. The relation is well expressed by a straight line which shows the tendency of the specific heat to increase with an increase in temperature.

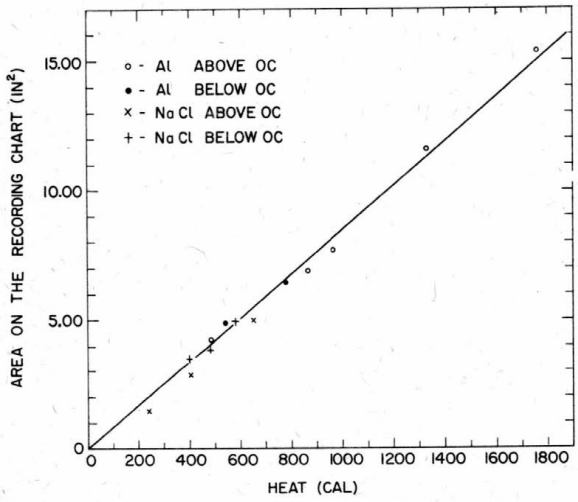

Figure 19. Calibration of the heat-transfer calorimeter.

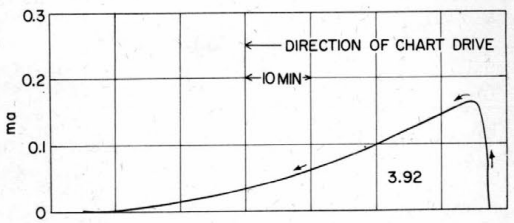

Figure 20. Sample chart record for measurement of specific heat, test 6.

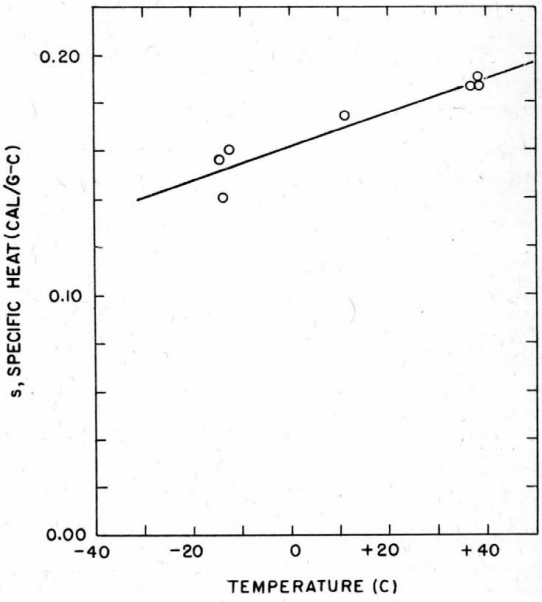

Figure 21. Specific heat of dry soil vs temperature.

Table VI. Specific heat of the soil.

	Test	Weight (g)	Temperature change and mean temp. (C)		Area on the chart (in^2)	Heat (cal)	Specific heat (cal/g-C)
Unfrozen soil with 2% moisture content	1	108.2	51.5	25.5 (38.5)	4.85	570	0.195
	2	130.4	51.5	22.9 (37.2)	6.71	786	0.193
	3	108.2	51.4	25.8 (38.6)	5.28	620	0.193
	4	103.0	22.8	1.0 (10.9)	3.92	464	0.187
Frozen soil with 1% moisture content	5	119.2	−6.0	−22.2 (−14.1)	2.89	344	0.178
	6	125.3	−1.9	−22.5 (−12.2)	3.92	464	0.180
	7	157.2	−4.3	−23.0 (−13.7)	4.25	502	0.170

Volume specific heat c_ρ of the frozen soil at various moisture contents, which is needed for determining the thermal conductivity, was calculated by the following equation:

$$c_\rho = s\gamma + iw\gamma \qquad (10)$$

where γ is dry density, s is specific heat of the dry soil, i is specific heat of the ice, and w is moisture content. The numerical value of s was determined as 0.155 cal/g-C at −10C on Figure 21 and the value of i was taken as 0.477 at −10C from tables of physical constants. Calculations for every 10% of moisture content are given in Table VII and the relationship is plotted on Figure 18. The dry density corresponding to each moisture content value in the table was taken from the actual saturation moisture curve in Figure 2. Below 20% moisture content, the dry density is constant.

Table VII. Volume specific heat of frozen soil.

w (%)	γ	$s\gamma$	$w\gamma$	$iw\gamma$	c_ρ
0	1.40	0.217	0.000	0.000	0.217
10	1.40	0.217	0.140	0.067	0.284
20	1.40	0.217	2.280	0.134	0.359
30	1.31	0.203	0.393	0.187	0.390
40	1.41	0.177	0.456	0.217	0.394
50	1.00	0.155	0.500	0.239	0.394
60	0.92	0.143	0.552	0.263	0.406
70	0.83	0.129	0.581	0.277	0.406
80	0.76	0.118	0.608	0.290	0.408
90	0.70	0.108	0.630	0.301	0.409
100	0.65	0.101	0.650	0.310	0.411
110	0.60	0.093	0.660	0.314	0.408
120	0.56	0.087	0.672	0.320	0.407
130	0.53	0.082	0.688	0.328	0.410
140	0.50	0.078	0.700	0.334	0.412
150	0.48	0.074	0.712	0.339	0.413
160	0.45	0.070	0.720	0.343	0.413
170	0.43	0.067	0.731	0.348	0.415
180	0.41	0.064	0.737	0.351	0.415
190	0.39	0.061	0.741	0.353	0.415
200	0.37	0.057	0.750	0.358	0.415

Volume specific heat of the unfrozen soil at saturation moisture content ($w = 24.5\%$, $\gamma = 1.45$) was calculated in a similar manner, using $s = 0.165$ at +5C and the specific heat of water s_w instead of the specific heat of ice in eq 10. This is calculated as follows:

$$\begin{aligned} c_\rho &= s\gamma + s_w w\gamma \\ &= 0.165\text{x}1.45 + 1.00\text{x}0.245\text{x}1.45 \\ &= 1.45\ (0.165 + 0.245) \\ &= 0.595 \end{aligned}$$

The thermal conductivity of the soil K by definition is $K = c_\rho \alpha$. Taking values of c_ρ and α from Figure 18, K of the frozen soil was computed for every 10% of moisture content (Table VIII). From the values obtained, a smooth curve is drawn on Figure 18 to show the relationship between the thermal conductivity of the frozen soil and the moisture content. The curve has a tendency of steepness similar to the curve of thermal diffusivity.

Thermal conductivity of the unfrozen soil at saturation moisture content is also calculated from $K = c_\rho \alpha$. Using the values of $c_\rho = 0.595$ cal/cm³-C and $\alpha = 4.02\text{x}10^{-3}$ cm²/sec as obtained above, K is calculated as $2.39\text{x}10^{-3}$ cal/cm-C-sec.

Table VIII. Thermal conductivity of frozen soil.

w%	α (cm²/sec)	c_ρ (cal/cm³—C)	K (cal/cm-C-sec)
0	$1.85\text{x}10^{-3}$	0.217	$0.401\text{x}10^{-3}$
10	2.95	0.284	0.837
20	3.97	0.355	1.410
30	4.92	0.388	1.910
40	5.68	0.400	2.272
50	6.32	0.402	2.540
60	6.83	0.405	2.768
70	7.23	0.407	2.941
80	7.58	0.408	3.093
90	7.88	0.409	3.222
100	8.12	0.410	3.330
120	8.51	0.411	3.497
140	8.82	0.412	3.633
160	9.09	0.413	3.754
180	9.32	0.415	3.867
200	9.53	0.415	3.956

ANALYSIS AND DISCUSSION

Thermal regime in frost heaving

Equipped with all the data which are needed to analyze the thermal regime in the soil while freezing, we can now treat the problem thermodynamically.

When the thermodynamic stage, that is to say the temperature distribution and the freezing process, is stable or quasi-stable, we can write the equation of heat balance at the freezing line in the soil as follows:

$$K_1 \frac{du_1}{dX} = K_2 \frac{du_2}{dX} + L_i w_s \gamma \frac{dX}{dt} + \frac{L_i}{v_i} \frac{d\xi}{dt} \cdot \qquad (11)$$

In this equation K is the thermal conductivity of the soil, du/dX is the temperature gradient at the freezing depth, L_i is the latent heat of ice, dX/dt is the penetration rate of the freezing line, v_i is the specific volume of ice and $d\xi/dt$ is the heaving rate. Subscripts 1 and 2 represent the frozen and unfrozen parts of the soil respectively. This equation indicates that, at the freezing line, heat flow to the surface through the frozen soil (material 1) should be equal to the heat flow from below through the unfrozen soil (material 2) plus the latent heat generated at the freezing line. This is illustrated schematically in Figure 22.

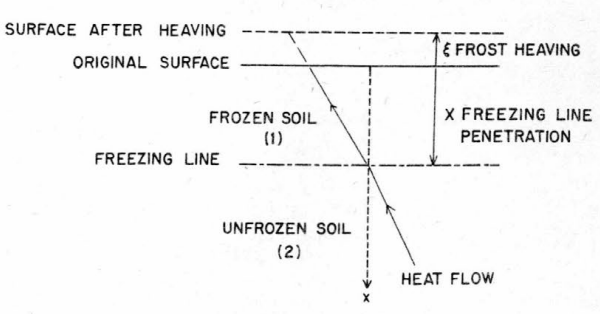

Figure 22. Schematic diagram of frost heaving.

Table IX. Relation between $d\xi/dt$ and $K_1 du_1/dX - K_2 du_2/dX$.

Sample	Date	$d\xi/dt$ (mm/day)	K_1 (cal/cm-C-sec)	du_1/dX (C/cm)	du_2/dX (C/cm)	$K_1 du_1/dX$ (cal/cm²-sec)	$K_2 du_2/dX$ (cal/cm²-sec)	$K_1 du_1/dX - K_2 du_2/dX$ (cal/cm²-sec)
5	26-27 July	6.0	3.00×10^{-3}	0.64	0.54	1.92×10^{-3}	1.36×10^{-3}	0.56×10^{-3}
"	30 "	4.5	3.46	0.60	0.59	2.08	1.41	0.67
"	2- 3 Aug.	1.75	2.77	0.67	0.67	1.85	1.60	0.25
7	26-27 July	5.0	3.01	0.60	0.50	1.80	1.20	0.60
"	30 "	7.5	3.48	0.72	0.68	2.50	1.48	1.02
"	2- 3 Aug.	3.0	2.77	0.64	0.64	1.77	1.58	0.24
16	2- 3 Nov.	3.5	2.66	0.58	0.51	1.54	1.10	0.44
17	12-13 Dec.	1.0	3.60	0.32	0.31	1.15	0.86	0.29
"	16-17 "	0.5	2.81	0.30	0.21	0.84	0.74	0.10
19	8 "	2.0	3.49	0.43	0.38	1.50	0.91	0.59
"	16-17 "	0.5	2.66	0.42	0.38	1.12	0.91	0.21
22	30 June	3.0	3.00	0.68	0.60	2.04	1.43	0.61
"	12 July	6.5	3.73	0.65	0.70	2.42	1.68	0.74
24	28-29 June	5.0	3.08	0.62	0.61	1.91	1.52	0.39
"	11 July	2.0	3.25	0.62	0.66	2.02	1.58	0.44

Latent heat can be divided into two parts. One part is the latent heat generated by the freezing of water between soil particles in the saturated condition. This is expressed in the second term of the right side of eq 11 , and it is obvious that this term has significance only at the freezing line penetration. The second part is the latent heat generated by the freezing of water which is transported to the freezing interface. As the segregated ice in the frozen soil is this part of the frozen water, it causes substantially all of the frost heaving. This latent heat quantity is expressed in the third term on the right side of eq 11.

Transposing terms, eq 11 is written as

$$\frac{d\xi}{dt} = \frac{v_i}{L_i}\left\{\left(K_1 \frac{du_1}{dX} - K_2 \frac{du_2}{dX}\right) - L_i w_s \gamma \frac{dX}{dt}\right\}. \quad (12)$$

This equation shows how the heaving rate is related to both the thermal regime in the soil and the penetration rate of the freezing line.

When dX/dt, the penetration rate of the freezing line, is large, a stable or quasi-stable state does not exist, because the temperature distribution is changing rapidly. Accordingly, quantitative analysis of the thermal regime based on eq 12 is possible only when dX/dt is approximately zero.

In this case eq 12 will be

$$\frac{d\xi}{dt} = \frac{v_i}{L_i}\left(K_1 \frac{du_1}{dX} - K_2 \frac{du_2}{dX}\right). \quad (13)$$

The condition $dX/dt \cong 0$ corresponds to the state in which the freezing line stays at a certain depth and an ice filament layer is growing. Hence eq 13 must hold as a relation between the heaving rate and the thermal regime in the soil. The validity of this equation was checked with the data whenever the value dX/dt approached or equaled zero. For calculation of $K_1 du_1/dX - K_2 du_2/dX$, temperature gradients were taken near the freezing line as the tangents to the temperature distribution curves, as described in the previous section.

Thermal conductivity of the frozen soil K_1 was determined from Figure 18 as a function of the moisture content of the frozen soil layer which lay just above the ice filament layer. For example, for the ice filament layer grown on 26-27 July in sample 7, K_1 was determined as the thermal conductivity of layer A (see photograph on Fig. 13). As this layer has a moisture content of 75%, Figure 18 shows that $K_1 = 3.01\times10^{-3}$ cal/cm-C-sec. For the unfrozen soil, $K_2 = 2.39\times10^{-3}$ cal/cm-C-sec, which was determined in the preceding section, was adopted. Data and the results of calculation are given in Table IX and the relationships between $d\xi/dt$ and the sensible heat loss $K_1 du_1/dX - K_2 du_2/dX$ are plotted in Figure 23.

The straight line on this graph is computed from eq 13, with its slope equal to v_i/L_i. Though scattered to some extent, the observed values are grouped reasonably well along the theoretical curve. This indicates that the heaving rate of the ice-filament layer is determined by the thermal

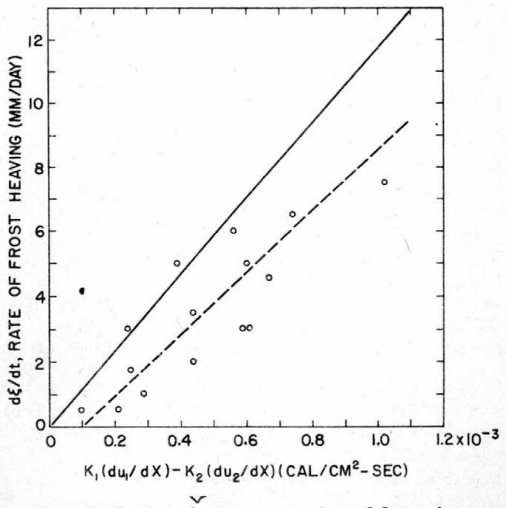

Figure 23. Relation between rate of heaving and sensible heat loss in ice filament layer formation.

regime in the soil. Deviation of the actual regression line (broken line) from the theoretical curve may be due to the fact that actual thermal conductivity of unfrozen soil is possibly larger than the measured value, because of the moisture movement which took place during the experiments.

Figure 23 shows that, in the case of the ice filament layer, the heaving rate changes over a wide range (0-7.5 mm/day) according to the amount of sensible heat loss $K_1\, du_1/dX - K_2\, du_2/dX$. One of the extreme cases in this range is when the sensible heat loss is zero. In this case the amount of heat transfer above and below the freezing line are balanced and no frost heaving can occur. This is a critical condition in the sense that, if the sensible heat loss becomes negative for any reason, melting will start at the freezing interface. Such a critical condition occurs when the air temperature on the soil surface is raised and reduces the temperature gradient in the frozen part.

The other extreme case develops when $d\xi/dt$ reaches a maximum for a given temperature condition. In the range of temperature and dry density covered in the experiments, 7.5 mm/day was the maximum heaving rate of the ice-filament layer and the corresponding theoretical value of the sensible heat loss was 0.62 cal/cm-sec. When the sensible heat loss exceeded this value, the excess loss caused the penetration of the freezing line and the thermal conditions enter into the region that produces freezing of the sirloin type. The maximum heaving rate in this region occurs when dX/dt is rather small and the maximum heaving rate is almost the same as that for the ice filament layer.

Consequently we can conclude that the most favorable condition for forming pure ice-filament layers lies between these two extremes, when thermal conditions produce a slightly lower heaving rate than the maximum rate for the sirloin type. This might explain the findings of Nakaya and Sugaya (1942) that the heaving rate of an ice filament layer was generally smaller than that of the sirloin type.

Relation between rate of frost heaving and rate of freezing line penetration

Results expressed in eq 9 may arouse considerable controversy because many investigators of frost heaving have hitherto concluded that the heaving rate is independent of the rate of freezing line penetration. The present author would like to offer a valid explanation of eq 9 and clarify the reasons which have led other investigators to different results.

It is generally agreed that the water used for ice segregation in the soil is drawn from below by some sort of suction force, although the nature of this force has not yet been explained. It is also agreed that this suction force must be due to the creation of ice in the frozen soil. Hence, we may assume that the suction force has a character analogous to a capillary force and thereby establish an equivalent height of water drawn up by this suction force, similar to a capillary height. The equation of the movement of water to the freezing line then becomes

$$q = ki = k\,\frac{h-z}{z} \qquad (14)$$

where

- k = permeability of the soil
- i = hydraulic gradient
- h = pressure head of the suction force
- z = distance between the freezing line and the ground water level
- q = flow rate of the water through a unit area

As the h is caused by the creation of ice at the freezing interface, it would be reasonable to assume that the magnitude of h is proportional to the area of the ice surface at the freezing line. The maximum value of h must then be expected in the case of ice-filament layer freezing, in which the boundary surface is entirely covered by ice. We shall designate the maximum value of h by h_m and the maximum value of q by q_m. This q_m is then the maximum possible rate at which water will be segregated as ice when the thermal conditions are favorable or, in other words, when the rate of removal of sensible heat is just enough to freeze this amount of water. If the rate of sensible heat loss is insufficient to freeze this amount, it will create an ice filament layer with a heaving rate which will be determined by eq 13.

When the rate of sensible heat removal exceeds the value which is just enough to freeze the water of q_m, the excess heat loss causes the freezing line to penetrate downwards. When this happens some soil particles are included and the ice surface area is reduced. This will decrease the magnitude of h, which we have assumed proportional to the ice surface area. The amount by which h is reduced will be proportional to the cross-sectional area occupied by the soil grains in the freezing plane.

Accordingly, h will be expressed as

$$h = h_m - \beta\left(1-n^{\frac{2}{3}}\right)\frac{dX}{dt}. \qquad (15)$$

Here n is porosity of the unfrozen soil, $(1 - n^{2/3})$ is the original ratio of the area occupied by the soil at the cross section, and β is a constant. Consequently, the flow rate of the water to the ice will be

$$q = \frac{k}{z}\left\{h_m - \beta\left(1-n^{\frac{2}{3}}\right)\frac{dX}{dt} - z\right\}$$

$$= \frac{k}{z}\left\{h_m - z - \beta\left(1-n^{\frac{2}{3}}\right)\frac{dX}{dt}\right\}$$

$$= q_m - \frac{k\beta}{z}\left(1-n^{\frac{2}{3}}\right)\frac{dX}{dt} \qquad (16)$$

which is the rate of ice segregation when the freezing line is penetrating at a rate of dX/dt, namely

$$\frac{d\xi}{dt} = q_m - \frac{k\beta}{z}\left(1-n^{\frac{2}{3}}\right)\frac{dX}{dt}. \qquad (17)$$

This equation is of the same type as eq 9.

As the numerical values of z or β were not determined in our experiments, we cannot verify eq 17 by checking the numerical values of A and B in eq 9. However, we can verify eq 17 comparatively for different values of k. We have two different values of A and B corresponding to two different densities in Table IV. As the permeability is a function of the dry density, the ratio of maximum heaving rates at different dry densities should be equal to the ratio of the permeabilities, namely the ratio of the two values of A in Table IV must be equal to the ratio of the permeabilities at dry density 1.25 and 1.45. Values of permeability were taken from Figure 3 and calculations are tabulated in Table X. Agreement of the ratios is fairly good. If the constant β is independent of the dry density, the ratio of the B's must be equal to the ratio of the two values of $k(1-n^{2/3})$. The calculations in Table X do not show as high a degree of coincidence as for the A's. However, we can see that eq 17 is verified semi-quantitatively by these comparisons.

It can now be shown why former investigators concluded that the heaving rate is independent of the rate of freezing line penetration. In all preceding investigations, the water table was kept just at the bottom of the soil sample. As the height of the sample is not great (10 - 20 cm), term z in the eq 16 is almost zero. This situation makes the term $(h_m - z)$ very large in comparison to $\beta(1-n^{2/3})dX/dt$ in eq (16). When the ground water level is kept just at the bottom of the sample, the heaving rate should be equal to the maximum rate as determined by the permeability and the suction pressure head and would not be affected by the rate of freezing line penetration.

In the author's experiments, the ground water level was separated from the bottom of the sample and the water was sucked up by a system of wicks. These wicks provided a distance between the soil and the ground water level that might be equivalent to several feet of soil. In this case z in eq 16 is fairly large, making the term $(h_m - z)$ comparable in magnitude to $\beta(1-n^{2/3})\ dX/dt$. This case is then governed by eq 17. Accordingly if we wish to simulate natural conditions in which the ground water level lies at a depth of several feet, we must adopt some method of simulating the depth of ground water level as the use of wicks in the present experiment.

The hydraulic condition described above must be in agreement with thermal conditions, because the ice segregation and the freezing line penetration expressed by eq 17 or 9 must hold thermally as well. Therefore, the following two equations must hold simultaneously;

$$\frac{d\xi}{dt} = A - \frac{B\,dX}{dt} \tag{9}$$

$$\frac{d\xi}{dt} = \frac{v_i}{L_i}\left\{\left(K_1\frac{du_1}{dX} - K_2\frac{du_2}{dX}\right) - L_i\gamma w_s\frac{dX}{dt}\right\}. \tag{12}$$

Combining these two equations, we can get the following relation:

$$\frac{dX}{dt} = \frac{1}{L_i\gamma w_s - B}\left\{\frac{v_i}{L_i}\left(K_1\frac{du_1}{dX} - K_2\frac{du_2}{dX}\right) - A\right\}. \tag{18}$$

Eq 18 shows that, when the sensible heat loss exceeds the optimum value described before, the excess heat loss causes the freezing line to penetrate downwards and the penetration rate is proportional to the excess amount of heat loss.

To check the relationship between dX/dt and the excess heat loss, a rough estimate of the excess heat loss was made, because of the difficulty in evaluating the sensible heat loss in a transient condition. A rough estimate was obtained by considering the drop in air temperature after each fairly long period of constant temperature. At the end of such a constant temperature period, the thermal condition of the soil corresponds to that needed for ice filament layer formation as shown by the frost penetration line on Figure 13. Accordingly, we can say that the drop in air temperature at the end of such periods indicates the excess heat loss which causes penetration of the freezing line. Taking the values of temperature drops from the time vs temperature curves, as in Figure 11, and measuring the corresponding rate of freezing line penetration on the graph, we obtain the temperature drop ΔT vs dX/dt relationship. The results are shown on Figure 24, and we can see that the linear relationship hold except in the range of small values of dX/dt. Hence, it is proved qualitatively that the hydraulic consideration described above can be consistent with thermal conditions.

Figure 24 is also useful for predicting the rate of freezing line penetration in relation to the change of air temperature. This might be a simple method to approximate the effect of the air temperature on the type of ice segregation in the soil, neglecting the complex nature of the thermal regime in the soil.

Table X. Semi-quantitative comparison of eq 9 with eq 17.

	A (mm/day)	Permeability k (cm^2/sec)	B	n %	$k(1-n^{2/3})$
(1) Values for $\gamma = 1.25$	7.4	0.70×10^{-4}	0.25	51.0	0.254×10^{-4}
(2) Values for $\gamma = 1.45$	4.2	0.40×10^{-4}	0.21	43.5	0.170×10^{-4}
Ratio of (1) to (2)	1.76	1.75	1.19		1.49

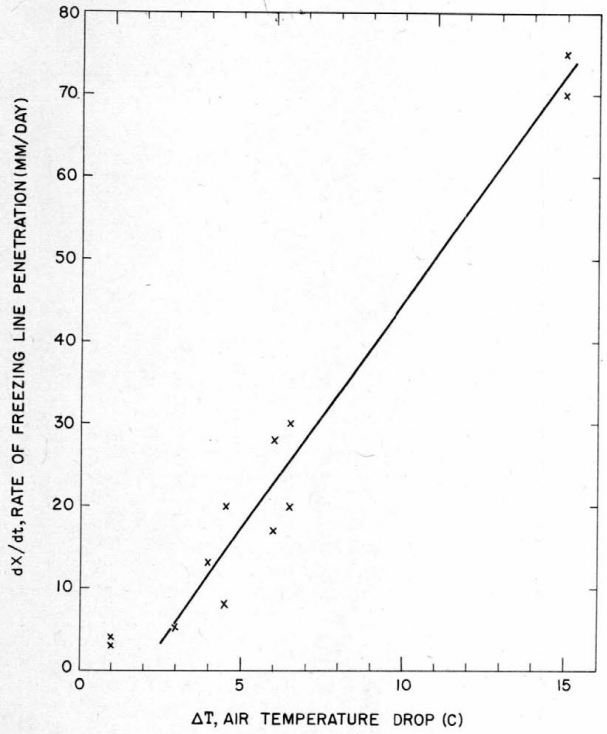

Figure 24. Rate of freezing line penetration vs air temperature drop after a long period of constant temperature.

CONCLUSION AND RECOMMENDATIONS

The results obtained in this experimental study are summarized as follows:

1. Moisture content of the frozen soil is related to the heaving ratio, inasmuch as the amount of frost heaving is attributed to the amount of segregated ice in the soil.

2. Types of ice segregation have been correlated with freezing line penetration as well as with frost heaving rate.

3. The frost heaving rate is related to the rate of freezing line penetration. This relationship is expressed by the equation

$$d\xi/dt = A - B\, dX/dt \qquad (9)$$

where the constants A and B are functions of the original dry density of the soil.

4. In the case of the ice-filament layer type of ice segregation, the heaving rate is determined by the amount of sensible heat loss at the freezing interface. The quantitative relationship between these quantities coincides well with the expected value from the equation of heat balance at the freezing interface:

$$\frac{d\xi}{dt} = \frac{v_i}{L_i}\left(K_1 \frac{du_1}{dX} - K_2 \frac{du_2}{dX}\right). \qquad (13)$$

5. When the amount of sensible heat loss exceeds the value which is necessary for a maximum heaving rate of the ice filament layer, the freezing line drops and the heaving rate obeys eq 9.

Further work is recommended to understand the phenomena of frost heaving from the hydraulic as well as the thermal point of view. For this purpose methods are needed to simulate natural depths of ground water level and natural soil permeabilities in small model experiments. It may be better to carry out experiments of actual size, which would permit good simulation of these conditions, though they would take a long time. Further study of the mechanism of water suction to the freezing line in the process of soil freezing is needed to establish a hydraulic law applicable to the case.

REFERENCES

Beskow, Gunnar (1935) Tjalbildningen och tjallyftningen med sarskild hansyn till vagar och jarnvagar (Soil freezing and frost heaving with special application to roads and railroads), The Swedish Geological Society, Series C, no. 375, 26th Year Book, no. 3, 145p.
(Translated by J. O. Osterberg, Technological Institute, Northwestern University, Evanston, Ill., Nov. 1947, with special supplement for the English translation of progress from 1935 to 1946.)

Frost Effects Laboratory, Corps of Engineers (1952) Investigation of description, classification, and strength properties of frozen soils, Snow, Ice and Permafrost Research Establishment, Corps of Engineers, U. S. Army, SIPRE Report 8, vol. I, p. 77 and pl. A2.

Haley, James F. (1953) Cold-room studies of frost action in soils, A progress report, Highway Research Board Bulletin No. 71 (Soil temperature and ground freezing) NAS-NRC, p. 1-18.

Higashi, Akira (1953) On the thermal conductivity of soil, with special reference to that of frozen soil, Transactions of the American Geophysical Union, vol. 34, p. 737-748.

_____and Murao, Tsuyoshi (1954) Improvement of the heat transferring calorimeter, Journal of Applied Physics, Japan, vol. 23, p. 127-129 (text in Japanese).

Nakaya, Ukichiro, and Magono, Choji (1940; 1942) On the mechanism of frost heaving, Pt. I, II, Journal of the Meteorological Society of Japan, vol. 18, p. 313-321; vol. 20, p. 125-136 (text in Japanese).

_____ Sugaya, Juji (1942) (Physics of frost heaving), Journal of Applied Physics, Japan, vol. 11, p. 160-165 (text in Japanese).

Yosida, Zyungo, and Wakiya, Shoich (1950) Heat-transfer calorimeter, Journal of Applied Physics, Japan, vol. 19, p. 226 (text in Japanese).

AD Accession No

U. S. Army Snow Ice and Permafrost Research Establishment, Corps of Engineers, Wilmette, Ill.
EXPERIMENTAL STUDY OF FROST HEAVING - Akira Higashi

Research Report 45, Aug 58, 44pp-illus-tables.
DA Proj 8-66-02-004, SIPRE Proj 22.3-3.
Unclassified Report

Laboratory studies on the effects of the soil-temperature regime on the type of ice segregation and the rate of frost heaving are described in detail, and the results are analyzed quantitatively on the basis of thermodynamic and hydraulic theory, assuming that suction is created by ice formation. The heaving rate varied with the type of ice segregation, which in turn depended on the rate of frost penetration. Ice-filament layers or sirloin-type freezing were observed at low penetration rates and concrete-type freezing at high penetration rates. The heaving rate decreased with increasing frost-penetration rate, and varied, in the case of filament-type freezing, according to the amount of sensible heat lost at

(over)

UNCLASSIFIED

1. Soils--Frost action effects
2. Soils--Freezing
I. Higashi, Akira
II. U.S. Army Snow Ice and Permafrost Research Establishment

AD Accession No

U. S. Army Snow Ice and Permafrost Research Establishment, Corps of Engineers, Wilmette, Ill.
EXPERIMENTAL STUDY OF FROST HEAVING - Akira Higashi

Research Report 45, Aug 58, 44pp-illus-tables.
DA Proj 8-66-02-004, SIPRE Proj 22.3-3.
Unclassified Report

Laboratory studies on the effects of the soil-temperature regime on the type of ice segregation and the rate of frost heaving are described in detail, and the results are analyzed quantitatively on the basis of thermodynamic and hydraulic theory, assuming that suction is created by ice formation. The heaving rate varied with the type of ice segregation, which in turn depended on the rate of frost penetration. Ice-filament layers or sirloin-type freezing were observed at low penetration rates and concrete-type freezing at high penetration rates. The heaving rate decreased with increasing frost-penetration rate, and varied, in the case of filament-type freezing, according to the amount of sensible heat lost at

(over)

UNCLASSIFIED

1. Soils--Frost action effects
2. Soils--Freezing
I. Higashi, Akira
II. U.S. Army Snow Ice and Permafrost Research Establishment

AD Accession No

U. S. Army Snow Ice and Permafrost Research Establishment, Corps of Engineers, Wilmette, Ill.
EXPERIMENTAL STUDY OF FROST HEAVING - Akira Higashi

Research Report 45, Aug 58, 44pp-illus-tables.
DA Proj 8-66-02-004, SIPRE Proj 22.3-3.
Unclassified Report

Laboratory studies on the effects of the soil-temperature regime on the type of ice segregation and the rate of frost heaving are described in detail, and the results are analyzed quantitatively on the basis of thermodynamic and hydraulic theory, assuming that suction is created by ice formation. The heaving rate varied with the type of ice segregation, which in turn depended on the rate of frost penetration. Ice-filament layers or sirloin-type freezing were observed at low penetration rates and concrete-type freezing at high penetration rates. The heaving rate decreased with increasing frost-penetration rate, and varied, in the case of filament-type freezing, according to the amount of sensible heat lost at

(over)

UNCLASSIFIED

1. Soils--Frost action effects
2. Soils--Freezing
I. Higashi, Akira
II. U.S. Army Snow Ice and Permafrost Research Establishment

AD Accession No

U. S. Army Snow Ice and Permafrost Research Establishment, Corps of Engineers, Wilmette, Ill.
EXPERIMENTAL STUDY OF FROST HEAVING - Akira Higashi

Research Report 45, Aug 58, 44pp-illus-tables.
DA Proj 8-66-02-004, SIPRE Proj 22.3-3.
Unclassified Report

Laboratory studies on the effects of the soil-temperature regime on the type of ice segregation and the rate of frost heaving are described in detail, and the results are analyzed quantitatively on the basis of thermodynamic and hydraulic theory, assuming that suction is created by ice formation. The heaving rate varied with the type of ice segregation, which in turn depended on the rate of frost penetration. Ice-filament layers or sirloin-type freezing were observed at low penetration rates and concrete-type freezing at high penetration rates. The heaving rate decreased with increasing frost-penetration rate, and varied, in the case of filament-type freezing, according to the amount of sensible heat lost at

(over)

UNCLASSIFIED

1. Soils--Frost action effects
2. Soils--Freezing
I. Higashi, Akira
II. U.S. Army Snow Ice and Permafrost Research Establishment

the freezing interface. The sensible heat loss was 0.62 cal/cm-sec in the case of maximum heaving (7 mm/day); higher values resulted in thermal conditions favoring sirloin-type freezing. The moisture content of frozen soil was found to be related to the heaving ratio, inasmuch as the amount of heaving is attributed to the amount of segregated ice.

the freezing interface. The sensible heat loss was 0.62 cal/cm-sec in the case of maximum heaving (7 mm/day); higher values resulted in thermal conditions favoring sirloin-type freezing. The moisture content of frozen soil was found to be related to the heaving ratio, inasmuch as the amount of heaving is attributed to the amount of segregated ice.

the freezing interface. The sensible heat loss was 0.62 cal/cm-sec in the case of maximum heaving (7 mm/day); higher values resulted in thermal conditions favoring sirloin-type freezing. The moisture content of frozen soil was found to be related to the heaving ratio, inasmuch as the amount of heaving is attributed to the amount of segregated ice.

the freezing interface. The sensible heat loss was 0.62 cal/cm-sec in the case of maximum heaving (7 mm/day); higher values resulted in thermal conditions favoring sirloin-type freezing. The moisture content of frozen soil was found to be related to the heaving ratio, inasmuch as the amount of heaving is attributed to the amount of segregated ice.